

[Click here to view linked References](#)

1 **Morpho-molecular traits of Indo-Pacific and Caribbean *Halofolliculina* ciliate infections**

1
2
3

4
5 3 Simone Montano¹⁻² *, Davide Maggioni¹⁻², Giulia Liguori¹⁻², Roberto Arrigoni³⁻⁴⁻⁵, Michael L.
6
7 4 Berumen⁵, Davide Seveso¹⁻², Paolo Galli¹⁻², Bert W. Hoeksema^{6,7}

8
9
10 5

11
12 6 ¹Department of Earth and Environmental Sciences (DISAT), University of Milan – Bicocca, Piazza
13
14 7 della Scienza, 20126, Milan, Italy.

15
16
17 8 ²MaRHE Center (Marine Research and High Education Center), Magoodhoo Island Faafu Atoll,
18
19 9 Republic of Maldives

20
21
22 10 ³Department of Biology and Evolution of Marine Organisms (BEOM), Stazione Zoologica Anton
23
24 11 Dohrn Napoli, Villa Comunale, 80121 Napoli, Italy

25
26
27 12 ⁴European Commission, Joint Research Centre (JRC), Ispra, Italy

28
29 13 ⁵Red Sea Research Center, Division of Biological and Environmental Science and Engineering, King
30
31 14 Abdullah University of Science and Technology, Thuwal 23955- 6900, Saudi Arabia

32
33
34 15 ⁶Taxonomy and Systematics Group, Naturalis Biodiversity Center, P.O. Box 9517, 2300 RA Leiden,
35
36 16 The Netherlands

37
38
39 17 ⁷Groningen Institute for Evolutionary Life Sciences, University of Groningen, P.O. Box 11103, 9700
40
41 18 CC Groningen, The Netherlands

42
43
44 19
45
46 20 *Corresponding Author: Simone Montano, Department of Earth and Environmental Sciences (DISAT), University of
47
48 21 Milan – Bicocca, Piazza della Scienza, 20126, Milan, Italy Milano. E-mail: simone.montano@unimib.it; phone:
49
50 22 +390264483433

51
52 23

53 **Abstract**

54
55
56
57 25 Coral diseases are emerging as a major threat to coral reefs worldwide and although many of them
58
59 26 have been described, knowledge on their epizootiology is still limited. This is the case of the

60
61
62
63
64
65

27 *Halofolliculina* ciliate infections, recognized as the Skeletal Eroding Band (SEB) and Caribbean
1
28 Ciliate Infection (CCI), two diseases caused by ciliates belonging to the genus *Halofolliculina* (Class
3
4
29 Heterotrichea). Despite their similar macroscopic appearance, the two diseases are considered
6
30 different and their pathogens have been hypothesised to belong to different *Halofolliculina* species.
8
9
31 In this work, we analysed the morphology and genetic diversity of *Halofolliculina* ciliates collected
10
11
12 in the Caribbean Sea, Red Sea, and Indo-Pacific Ocean. Our analyses showed a strong macroscopic
13
14
33 similarity of the lesions and similar settlement patterns of the halofolliculinids from the collection
15
16
17
34 localities. In particular, the unique erosion patterns typical of the SEB were observed also in the
18
19
35 Caribbean corals. Fine-scale morphological and morphometric examinations revealed a common
20
21
22
36 phenotype in all analysed ciliates, unequivocally identified as *Halofolliculina corallasia*.
23
24
37 Phylogenetic analyses based on nuclear (ITS) and mitochondrial (COI) molecular markers
25
26
27
38 consistently found all samples as monophyletic. However, although the nuclear marker displayed an
28
29
39 extremely low intra-specific diversity, consistent with the morphological recognition of a single
30
31
40 species, the analyses based on COI showed a certain level of divergence between samples from
32
33
34
41 different localities. Genetic distances between localities fall within the intra-specific range found in
35
36
42 other heterotrich ciliates, but they may also suggest the presence of a *H. corallasia* species complex.
37
38
39
43 In conclusion, the presented morpho-molecular characterization of *Halofolliculina* reveals strong
40
41
42 similarities between the pathogens causing SEB and CCI and call for further detailed studies about
43
44
45 the distinction of these two coral diseases.

46
47
48
49
50
51
52
53
54
55
56
57
58
59
60
61
62
63
64
65

Keywords: ciliate, protozoan, syndrome, *Halofolliculina corallasia*, coral reefs, scleractinian corals

Introduction

52 Coral reefs are declining worldwide, with an estimated coral cover loss of 50% in the Indo-Pacific
1
53 and 80% in the Caribbean over the last 30 years (Gardener et al. 2003; Bruno and Selig 2007; Pollock
3
54 et al. 2011). The causes of this decline are multiple and complex, with coral diseases emerging as one
4
6 of the most affecting threats (Rosenberg et al. 2007; Bourne et al. 2009; Sutherland et al. 2015).
7
8
9
10 56 Currently, it is not clear how many coral diseases exist globally, and a certain level of confusion
11
12 57 emerges from the incomplete information reported in the literature (Willis et al. 2004). Indeed, despite
13
14 58 their negative impact, the majority of coral diseases remain a mystery, as a result of the limited
15
16 59 analytic methods, the poor knowledge of the putative pathogens and the consequent deficiency of
17
18 60 epizootiological data (Work and Meteyer 2014; Bourne et al. 2015). One of the most dramatic and
19
20 61 recent examples is the Stony Coral Tissue Loss Disease (SCTLD), which has been affecting various
21
22 62 coral species along the Florida Reef Tract since 2014 (Aeby et al. 2019). Although its effect is
23
24 63 unprecedented, all the efforts carried out by research have so far not been successful in discovering
25
26 64 its causative agents (Meyer et al. 2019). The lack of specific and accurate diagnostic tools coupled
27
28 65 with difficulties encountered in the study of bacteria-based diseases resulted also in ambiguous
29
30 66 classifications of coral diseases that remain largely open to interpretation (Pollock et al. 2011). The
31
32 67 shortage of multidisciplinary approaches to describe coral lesions and to identify morphologically
33
34 68 and molecularly the pathogens have led to recognize a high number of possibly different diseases,
35
36 69 which often share similar gross morphology of the lesions, as for the Indo-Pacific White Syndromes
37
38 70 (Bourne et al. 2015). Furthermore, in some cases diseases were named differently, even if caused by
39
40 71 the same putative pathogens. This is the case of the Black Band Disease (BBD) and the Red Band
41
42 72 Disease (RBD) of Palau, in which the filamentous cyanobacteria forming red and black bands were
43
44 73 molecularly identified as belonging to a single ribotype only after their isolation, culturing and
45
46 74 sequencing (Sussman et al. 2006). Moreover, this scenario is further complicated by the existence of
47
48 75 coral diseases caused by a consortium of pathogens that may slightly differ among geographic areas.
49
50
51
52
53
54
55
56
57
58
59
60
61
62
63
64
65

77 microorganism dominated by a cyanobacterial component, may differ in its predominant portion
1
28 between the Caribbean and Indo-Pacific (Casamatta et al. 2012).
3
4
79 The Skeletal Eroding Band (SEB) is one of the first coral diseases detected and described from the
6
80 Indo-Pacific coral reefs (Antonius 1999). It is caused by the folliculinid ciliate *Halofolliculina*
8
9
81 *corallasia* Antonius and Lipscomb, 2001 (Class Heterotrichea; Order Heterotrichida), which not only
10
11
82 attacks the soft tissues of corals but also damages their skeleton (Antonius and Lipscomb 2001; Riegl
13
14
83 and Antonius 2003; Page and Willis 2008). In *H. corallasia*, the lorica (sac-like housing) has a
15
16
84 rounded posterior and a cylindrical neck that angles up from the surface at about 45°, and it has an
18
19
85 average length and width of 220 µm and 95 µm, respectively. They are settled on the coral skeleton,
20
21
86 usually following the rim of the corallites, and in most cases only the neck rises above the coral
22
23
87 surface. The disease manifests as a dark-grey band 1–10 cm thick, located at the interface between
25
26
88 recently exposed skeleton and apparently healthy coral tissue. The SEB has been recorded affecting
27
28
89 82 scleractinian species on various Indo-Pacific and Red Sea coral reefs, with the most affected taxa
30
31
90 being branching species of *Acropora* and *Pocillopora* (Page et al. 2015). According to these data, the
32
33
91 SEB shows the widest host range of any coral disease recorded to date, reaching the top on the list of
35
36
92 harmful coral syndromes (reviewed by Page and Willis 2008).
37
38
93 In 2004-2005, a similar ciliate infection was reported from 25 out of about 60 Caribbean coral species
40
41
94 (Cróquer et al. 2006a; Page et al. 2015), in which the infection appeared as a dark band located
42
43
95 between healthy tissue and bare skeleton, showing, on closer inspection, the characteristic spotted
44
45
96 appearance of the clustering ciliates (Cróquer et al. 2006a). The general morphology of the Caribbean
47
48
97 ciliate is very similar to that of *Halofolliculina corallasia* from the Indo-Pacific (Cróquer et al.,
49
50
98 2006b, Rodriguez et al. 2009). Both ciliates have a free-living phase that moves toward living tissues,
52
53
99 penetrates them and attaches itself, and a sessile form settled in a lorica, with the cell body attached
54
55
100 at its pointed posterior end, showing two conspicuous pericytostomial wings bearing feeding cilia
56
57
101 (Antonius, 1999; Antonius and Lipscomb, 2001; Cróquer et al., 2006b).
59
60
61
62
63
64
65

102 Despite a similar fine-scale morphology among *Halofolliculina* ciliates affecting Indo- Pacific and
1
103 Caribbean corals, the skeletal erosion is often associated with SEB, but not with the Caribbean ciliate
3
104 infections to date (Page et al. 2015). However, no information is present in the literature about the
4
6
105 apparent no-eroding pattern of ciliate affecting Caribbean corals, leaving space for additional in-depth
8
106 studies.

107 Initially, it was proposed that these ciliates might have recently invaded the Caribbean from the Indo-
13
108 Pacific region (Cróquer et al. 2006b), but then the authors stated that the Caribbean and Indo-Pacific
14
15
109 ciliates are different species, based on unpublished data (Cróquer et al. 2006a). Despite the Caribbean
16
18
19
110 pathogen is still to be formally characterised and described at species level, researchers suggested the
20
21
111 name Caribbean Ciliate Infections (CCI) to indicate the presumed new disease, due to the apparent
22
23
112 differences in aetiology (Weil and Hooten 2008; Rodríguez et al. 2009; Weil and Rogers 2011). By
24
25
113 contrast, it has also been reported by Sweet and Serè (2016) that SEB and CCI are caused by the same
26
27
114 pathogen, despite an absence of evidence to support this conclusion.
28
30

115 Therefore, the goal of this study is to improve the knowledge concerning the *Halofolliculina* Ciliate
31
32
33
116 Infections (*sensu* Page et al. 2015) by investigating the aetiology of SEB and CCI through a morpho-
34
35
117 molecular approach, in order to assess and confirm possible taxonomic affinities between the
36
37
118 *Halofolliculina* species.
38
40

119 120 **Material and methods**

121 Sampling was conducted between June 2017 and October 2019 in three geographic areas, including
42
43
122 the Indian Ocean (Republic of the Maldives), the Red Sea (Saudi Arabia) and the Caribbean Sea
44
45
123 (Curaçao and Bonaire) (Fig. 1).
46
47
48
49

124 The presence of the *Halofolliculina* Ciliate Infection was qualitatively recorded both by snorkeling
50
51
125 and SCUBA diving through a roving technique (Hoeksema and Koh, 2009). A dive of
52
53
126 approximately one hour was carried out at each sampling locality, starting from a maximum depth
54
55
56
127 of 10–25 m and moving towards shallower waters. In each locality, two to four small diseased coral
57
58
59
60
61
62
63
64
65

128 fragments were taken with a hammer and chisel from colonies showing the characteristic band.
1
129 Underwater photographs were taken using a Canon GX7 Mark II camera in a Fantasea GX7 II
3
130 underwater housing. Diseased coral colonies used in the study were chosen randomly (depending on
4
5
6
131 their abundance) and include *Pocillopora* spp. and *Porites lutea* in the Indo-Pacific and the Red Sea,
8
9
132 and *Eusmilia fastigiata* and *Diploria labyrinthiformis* in the Caribbean Sea. After a preliminary
10
11
133 observation, samples were fixed in formalin 6% and ethanol 99%, for further morphological and
13
14
134 molecular analyses, respectively.
15
16
135 Halofolliculinid protozoans were initially observed *in vivo* with a Leica EZ4 D stereomicroscope to
18
19
136 examine the protozoan aggregations and to search for possible macroscopic differences, such as a
20
21
137 different colouration and the shape of the lorica. Then, single individuals were detached from the
22
23
138 coral skeleton using needles, precision forceps and micropipettes and placed on a glass slide to
25
26
139 observe their morphology at higher magnification under a Zeiss Axioskop 40 microscope.
27
28
140 Subsequently, ten coral fragments belonging to the four genera (*Diploria*, *Eusmilia*, *Pocillopora*,
30
31
141 *Porites*) were observed using both the Tescan Vega TS 5136 XM scanning electron microscope,
32
33
142 operating at beam energies of 20kV, and the Zeiss Gemini SEM500 scanning electron microscope
35
36
143 operating at beam energies of 5kV. About 30 loricae were randomly chosen for each coral fragment
37
38
144 to take measurements of the diameter, length and width of both the neck and the ampulla, according
40
41
145 to Antonius and Lipscomb (2001) and Primc-Habdija et al. (2005) (Fig. S1). Measurements were
42
43
146 recorded using the Scanning Electron Microscope measuring software SmartSEM (ZEISS,
44
45
147 Oberkochen, Germany) with maximum resolution of 1 nm. Additionally, a preliminary
47
48
148 characterisation of the skeletal erosion caused by the CCI has also been carried out through SEM
49
50
149 imaging.
52
53
150 The morphometric measurements were tested for normality distribution with a Shapiro-Wilk test of
54
55
151 normality. One-way analyses of variance (ANOVA) were performed to test for differences in the
57
58
152 neck diameter between localities, whereas differences in the length of the neck and diameter of the
59
60
153 neck brim were tested using a non-parametric Kruskal-Wallis test, since the data were not normally
62
63
64
65

154 distributed (Zar 1999). Ampullae length and width of *Halofolliculina* loricae were analysed by
1
155 descriptive statistics due the few observations obtained. Statistical analyses were performed using
3
156 SPSS ver. 24 (IBM, New York). All data are presented as mean \pm standard error (SE), unless
6
157 otherwise stated.
8

158

159 ***Molecular analyses***

160 The genomic DNA was extracted following a protocol already successfully used for different taxa
161 (Montano et al. 2015; Beli et al. 2018). Two molecular markers were amplified, namely a portion of
162 the nuclear ITS (~400 bp) and the mitochondrial COI gene (~600 bp), following the protocols
163 described in Fernandes et al. (2016) and Strüder-Kypke and Lynn (2010), respectively. These two
164 DNA regions were chosen because they are generally considered reliable markers to infer ciliate
165 phylogeny (e.g. Sun et al. 2010; Yi and Song 2011; Fernandes et al. 2016) and because they show
166 different substitution rates, with the COI being the more variable marker and having been already
167 used to assess ciliates intra-specific variability (e.g. Gentekaki and Lynn 2009; Strüder-Kypke and
168 Lynn 2010). The amplicons were purified and sequenced in both forward and reverse directions using
169 a DNA Analyser 3730xl (Applied Biosystems, California, USA). The obtained sequences were
170 imported, assembled, and visually checked into Geneious R7. For each molecular marker, a dataset
171 was assembled adding sequences belonging to halofolliculind relatives downloaded from GenBank.
172 Sequences from two karyorelictid species (*Corlissina maricaensis*, *Loxodes vorax*) were also
173 included as outgroups. Sequences were aligned using the E-INS-i option in MAFFT 7.402 (Kato
174 and Standley, 2013), and were then run through Gblocks (Castresana 2000; Talavera and Castresana,
175 2007) to remove low quality and ambiguously aligned positions. Phylogenetic analyses were
176 performed using Bayesian Inference (BI) and Maximum Likelihood (ML). JmodelTest2 2.1.6
177 (Darriba et al., 2012) was run to find the proper molecular models, and the best-fitting model selected
178 for both datasets was GTR+G, as suggested by the Aikaike Information Criterion (AIC). BI analyses
179 were performed using MrBayes 3.2.6 (Ronquist et al., 2012): four parallel Markov Chain Monte Carlo

180 runs (MCMC) were run for 10^7 generations, trees were sampled every 1000th generation, and burn-
1
181 in was set to 25%. ML analyses were performed with RAxML v8.2.10 (Stamatakis, 2006, 2014)
2
3
4
182 using 1000 bootstrap replicates. Resulting trees were displayed and edited using FigTree 1.4.0
5
6
183 (Rambaut, 2012) and CorelDraw X7 (Corel Corporation, Ottawa, Canada). Genetic distances
7
8
9
184 (uncorrected *p*-distances, 1000 bootstrap) among and within heterotrich lineages were obtained for
10
11
185 both molecular markers using MEGA-X (Kumar et al., 2018). The obtained sequences were deposited
12
13
14
186 in GenBank (accession numbers ITS: MN829871-MN829873; COI: MN905752-MN905758) with
15
16
187 relative sample codes and sampling sites.
17
18
188

189 **Results**

190 ***Morphological results***

191 Our ecological surveys reveal the presence of *Halofolliculina* Ciliate Infections diseases in all three
192 investigated areas. First examinations revealed clusters of protozoans placed on coral surface between
193 recently exposed skeleton and apparently healthy coral tissues, forming dense bands characterised by
194 a dark green, almost black, colour pattern in diseased corals from both the Caribbean and the Indo-
195 Pacific (Fig. 2 a-b). In all samples, protozoans matched the description of *Halofolliculina corallasia*
196 provided by Antonius and Lipscomb (2000). The body was covered by rows of cilia and showed the
197 two characteristic bifurcate pericystomial wings bearing the oral polykinetids (Fig. 2 c-d).

198 To better visualize the morphology of the loricae and to confirm their identification, a total number
199 of 109 loricae (24 on *Porites lutea*, 29 on *Eusmilia fastigiata*, 10 on *Diploria labyrinthiformis*, 35 on
200 *Pocillopora damicornis*, and 11 on *Pocillopora verrucosa*) were examined using the SEM. All the
201 loricae had a rounded posterior and a cylindrical neck with a single sculpture line circumscribing it
202 (Fig. 3). Furthermore, no significative differences in the overall distribution, settlement patterns and
203 general size of the loricae have been observed between the coral genera and localities investigated.

204 In general, the mean ampulla length (*l*) and width (*w*) were higher in the Caribbean samples (*l*= 146.4
205 ± 4.3 μm; *w*= 83.3 ± 6.2 μm) compared to the Maldivian specimens (*l*= 112.7 ± 4.1 μm; *w*= 62.1 ±

206 4.7 μm) and the Red Sea specimens ($l= 54.3 \mu\text{m}$; $w= 51.1 \mu\text{m}$). Regarding the length of the neck,
1
207 mean values of $40.1 \pm 1.0 \mu\text{m}$ and $40.9 \pm 3.1 \mu\text{m}$ were observed in the Maldivian and Red Sea
3
208 specimens, respectively, whereas a mean value of $32.2 \pm 1.1 \mu\text{m}$ was observed for the Caribbean
4
6
209 ciliates. Furthermore, similar values were found for the neck diameter, with Maldivian, Red Sea and
8
210 Caribbean ciliates showing mean values of $31.25 \pm 0.9 \mu\text{m}$, $32.28 \pm 0.9 \mu\text{m}$ and $31.20 \pm 1.0 \mu\text{m}$,
10
211 respectively (Fig. 4).
13

14
212 According to the parametric and non-parametric tests performed, the neck diameters and neck lengths
15
213 were not statistically different between the three geographic areas (neck diameters: ANOVA
16
214 $F_{2,90}=0.406$, $p=0.668$; neck length: Kruskal-Wallis $H=6.06$ $p = 0.051$). In contrast, a significant
20
215 difference was observed for the neck brim diameter between the three geographic areas, with the
21
23
216 Maldivian specimens showing a mean value of $42.2 \pm 1.4 \mu\text{m}$, the Red Sea of $45.5 \pm 1.0 \mu\text{m}$ and the
25
217 Caribbean of $46.9 \pm 1.3 \mu\text{m}$ (Kruskal-Wallis $H=8.38$ $p = 0.015$). Maximum and minimum
26
28
218 morphometric data of the loricae from each of the geographic areas are summarized in Table S1.
30

31
219 In addition, peculiar micro-alterations have been identified on the surface of the skeleton of the
32
33
220 Caribbean scleractinian genera at locations where *Halofolliculina* ciliates were present (Fig. 5a). The
35
221 ciliates appear to modify the growth pattern of the host coral, apparently eroding part of the skeleton
36
37
38
222 and producing a round-shaped trace where the ciliates were located (Fig. 5 b-c). This results in distinct
40
223 footprints or marks on the coral surface attributable to the protozoans settlement. The shape of the
42
224 footprint appears cylindrical, although generally not regular, with a diameter ranging from about 50
43
45
225 μm in width to 95 μm in length (Fig. 5d). In some coral colonies a less evident eroded pattern,
47
226 ascribable to the presence of the loricae on the skeleton was also observed (Fig. 5 e-f).
48
49

227 228 ***Molecular results***

229 The total alignments of the ITS and COI datasets after the Gblocks treatment were 455 and 688 bp
57
230 long, and consisted in 36 and 40 sequences, respectively. BI and ML analyses resulted in almost
59
231 identical phylogenetic trees, and therefore only the ML topologies are shown in Fig. 4, with nodal
60
61
62
63
64
65

232 supports indicated as Bayesian posterior probabilities (BPP) and bootstrap supports (BS). The ITS
1
233 tree (Fig. 6a) shows an overall moderate to good nodal support for the Bayesian analysis, whereas
2
3
4
234 the ML analysis resulted in less supported relationships. All included genera are monophyletic, but a
5
6
235 few species are not. The *Halofolliculina* sequences obtained from different localities form a
7
8
9
236 monophyletic clade (BPP = 0.88, BS = 89), sister to *Folliculina simplex* (BPP = 0.99, BS = 84), the
10
11
237 only other folliculinid included in the analysis. The evolutionary relationships represented in the COI
12
13
14
238 tree (Fig. 6b) show higher support values for both BI and ML analyses at genus and species level, but
15
16
239 deeper nodes are generally less supported. However, all genera and species included in the analysis
17
18
19
240 are monophyletic, including the *Halofolliculina* clade (BPP = 1, BS = 100). In comparison to the ITS
20
21
241 analyses, the halofolliculinids collected from different localities show a higher diversification, and
22
23
242 three geography-related, fully supported lineages can be identified.

243 Genetic distances calculated between heterotrich species and genera are generally high, especially for
24
25
244 the COI dataset (Table S2). The average distances between genera and species for the COI dataset
26
27
28
29
245 are 39.9% (28.5 - 58.5%) and 32% (8.6 - 59.1%), respectively, with *Halofolliculina* showing the
30
31
32
33
246 highest distances towards all other sequences (Table S2). Distances between genera and species in
34
35
36
247 the ITS dataset are lower, being 21.8% (13.1 - 38.7 %) and 18% (0.4 - 39.4%), respectively (Table
37
38
39
248 S2). The intra-specific distances are higher for the COI dataset, ranging from 0 to 14%, whereas they
40
41
42
249 are lower for the ITS dataset (0.1 - 7.3%) (Table S2). Regarding the *Halofolliculina* sequences, intra-
43
44
250 genus distances are moderately high for the COI ($14 \pm 0.9\%$), but very low for the ITS (0.5 ± 0.4).
45
46
251 The genetic distances between *Halofolliculina* samples from the three localities are high, ranging
47
48
252 from 18.6 to 21.1% (Table S2).
49
50

253

254 Discussion

255 The present work reveals the relationship between *Halofolliculina* ciliate infections known as Skeletal
56
57
256 Eroding Band in the Indo-Pacific and as Caribbean Ciliate Infection in the Caribbean, by the
58
59
60
61
62
63
64
65

257 application for the first time, of an integrative, morphological-molecular approach. Coral lesions and
1
258 protozoans in the three geographic areas showed the same macroscopic appearance.
2
3
4
259 In all investigated affected coral species, halofolliculinid infestations manifested themselves as areas
5
6
260 of tissue loss and bare skeleton covered by loricae. *Halofolliculina* ciliates settle in clusters following
7
8
261 the rim of the corallites and represent dark dots, giving the skeleton a scattered appearance. When in
9
10
11
262 high densities they form a thick band (1-10 cm), usually black or dark green in colour, between
12
13
14
263 recently exposed skeleton and dead tissue. They can also form more speckled bands when in low
15
16
264 density and be more light green in colour. Thus, the *in vivo* observation of halofolliculinids confirmed
17
18
19
265 the previous information reported for the Skeletal Eroding Band disease (Antonius and Lipscomb
20
21
22
266 2000; Winkler et al. 2004; Page and Willis 2008) and the Caribbean Ciliate Infection (Croquer et al.
23
24
25
267 2006a). In particular, the analysis of the main features of the protozoans' body and lorica matched
26
27
28
268 with the description of *Halofolliculina corallasia* provided by Antonius and Lipscomb (2000) for all
29
30
31
269 specimens analyzed. Moreover, a detailed analysis of the skeleton revealed an erosion on Caribbean
32
33
34
270 diseased corals, suggesting for the first time settlement patterns similar to those of Indo-Pacific SEB-
35
36
271 affected corals. In particular, slightly eroded marks related to the presence of *Halofolliculina* loricae
37
38
39
272 have been observed on the Caribbean skeletons, revealing that the ciliate may use the same
40
41
42
273 mechanisms as in Indo-Pacific SEB-causing ciliates. Indeed, the Caribbean *Halofolliculina* ciliates
43
44
45
274 seems to manifest an apparently chemical activity by leaving "sack-shaped" borings or an
46
47
48
275 "honeycomb" pattern while attach their bodies on the coral skeleton as already reported for the Indo-
49
50
51
276 Pacific counterpart (Riegl and Antonius 2003). The footprints were consistent with the position and
52
53
54
277 size of the loricae of *H. corallasia*, although apparently different erosion degree within the same
55
56
57
278 samples or host has been detected. If this is related to the time they remain attached to the coral hosts
58
59
60
279 or if some other unknown factors are involved needs to be elucidated in future research.
61
62
63
280 The main character used to distinguish *H. corallasia* from its congeners is the presence of a single
64
65
66
281 sculpture line circumscribing the neck of the lorica (Antonius and Lipscomb 2000; Page et al. 2015).
67
68
69
282 The single line was evident and easily detectable in all examined protozoans from the Indo-Pacific,
70
71
72
73
74
75

283 Red Sea, and the Caribbean. In addition, all the obtained measures fall within the ranges estimated
1
284 for *H. corallasia* in its first description (Antonius and Lipscomb 2000). Statistical analyses revealed
2
3
4
285 no significant differences in the neck diameter and length, supporting the fine-scale morphological
5
6
286 similarities of halofolliculinids from the Caribbean and Indo-Pacific. Although a statistical difference
7
8
287 was found in the neck brim diameters, we believe this morphological character needs further
9
10
11
288 investigation since, in a few cases, loricae were distorted mainly due to the conservation of the sample
12
13
14
289 and to the great variability in the extensibility of the lorica (Primc-Habdija and Matoničkin, 2005),
15
16
290 and this may have introduced a bias in the measurements. Therefore, all individuals have
17
18
291 morphologically been identified as *H. corallasia*, and protozoans found in the Caribbean appeared to
19
20
21
292 be identical to those causing the SEB in the Indo-Pacific and Red Sea.
22
23
293 Overall, the understanding of the genetic relationships among ciliates is complicated by the
24
25
26
294 incomplete knowledge of their diversity (Strüder-Kypke and Lynn, 2010). Indeed, ciliated protozoans
27
28
295 are largely underrepresented in current biodiversity estimates for many reasons, such as their small
29
30
31
296 size and the difficulty in their isolation and culture (Kher et al., 2011). In line with this gap of
32
33
297 knowledge, no genetic information on *H. corallasia* and the whole genus *Halofolliculina* has been
34
35
298 presented so far in the literature and no sequences have been deposited in public databases.
36
37
299 Consequently, the DNA sequences herein obtained are the first molecular data for the entire
38
39
40
300 *Halofolliculina* genus and represent a starting point for future genetic evaluations of the species and
41
42
43
301 related taxa.
44
45
302 The molecular results partially diverge from the morphological characterization, finding relevant
46
47
48
303 differences between protozoans from different localities. Although both nuclear and mitochondrial
49
50
304 molecular markers revealed the monophyly of all *H. corallasia* individuals sequenced in this work,
51
52
305 ITS and COI markers showed variable levels of variation in protozoans from different localities. The
53
54
306 *H. corallasia* intra-specific genetic distance based on the ITS dataset was extremely low, whereas
55
56
307 that based on COI was higher. Moreover, genetic distances between *Halofolliculina* from the three
57
58
59
308 different localities were remarkably high. These results agree with previous works on ciliate genetic
60
61
62
63
64
65

309 diversity, in which COI showed a much higher diversification than the ITS region (Gentekaki and
1
310 Lynn 2009; Fernandes et al. 2016).
3
4
311 According to these molecular results, we may hypothesize two main opposite scenarios. Firstly, we
6
312 may be dealing with a single species with a circumtropical distribution. Indeed, the high intra-
8
313 *Halofolliculina* genetic distances observed for the COI fall within the range of intra-specific distances
10
314 found for other heterotrich species. The inter-specific divergence is generally much higher in ciliates
13
315 than in animals and the genetic distance thresholds used for species delimitation differ greatly among
14
316 ciliate taxa, being for instance around 1% for *Tetrahymena* spp. and 18% for *Carchesium* spp., based
16
317 on the COI (Gentekaki and Lynn, 2009; Kher et al., 2011). These data suggest that evolution rates
20
318 can be extremely high in ciliates, and that their intra-specific genetic diversity can vary largely among
21
319 taxa and could be taxon-specific (Gentekaki & Lynn, 2009; Strüder-Kypke and Lynn, 2010).
25
320 Researchers have suggested that a high ciliate genetic diversity can depend on several factors, such
26
321 as a strong gene flow and the ability of the dispersal phase of these microorganisms to reach large
30
322 distances (Gentekaki and Lynn, 2009). It is also assumed that, in population of ciliates highly isolated
31
323 from each other, a positive correlation exists between their genetic divergence and the geographic
33
324 distance, such as in the case of *Carchesium polypinum* (Templeton and Georgiadis, 1996; Zhang et
36
325 al., 2006). However, there still is no universal consensus about the possible biogeographic
38
326 diversification of ciliates. Even if rarely, in some cases ciliates population have been demonstrated to
40
327 have a genetic structure related to their biogeography (Miao et al. 2004; Katz et al. 2005), and this
42
328 may also the case of *H. corallasia*.
43
44
45
46
47
48
329 A second scenario would be the presence of multiple cryptic species with a similar morphology, as
49
50
330 already found also in other ciliates (e.g. Strüder-Kypke and Lynn 2010; McManus et al. 2010; Kats
52
331 et al. 2011; Park et al. 2019). In this latter case the ITS region would result as inappropriate to
53
332 distinguish between closely related species, whereas the COI divergence could be explained by the
54
55
333 presence of different species living in the three localities. Indeed, the COI genetic distances within
57
58
334 *H. corallasia* are comparable or higher than the interspecific divergences within the other genera
59
60
61
62
63
64
65

335 included in the analyses and show, for instance, patterns similar to those of some *Blepharisma*
1
336 species, which are well resolved with COI but not with ITS sequences. Moreover, Maldivian samples
3
4
337 are more similar to Caribbean ciliates rather than the Red Sea ones. This seems to contradict the
5
6
338 scenario of a circumtropical species with a biogeography-related genetic structure and further support
7
8
339 the species complex hypothesis.
9
10
340 Therefore, the morphological and molecular data obtained in this work seem to support more the
11
12
341 latter scenario, with the identification of a *H. corallasia* species complex as the pathogen associated
13
14
342 to both the Caribbean Ciliate Infection and Skeletal Eroding Band. Even though it cannot be excluded
15
16
343 that the SEB may be sympatric with the CCI in some localities, this would represent an unlikely
17
18
344 scenario. The most cautious approach when describing coral diseases would be to proceed with the
19
20
345 classification of different syndromes only when clear evidence is presented (Bourne et al. 2015).
21
22
346 Since we found an approximately identical morphology at micro- and macro-scale in ciliates and
23
24
347 lesions from different localities and since *H. corallasia* may actually be a complex of multiple cryptic
25
26
348 species, we believe that in order to reduce further confusion supplementary studies that will clarify if
27
28
349 CCI and SEB should be synonymized are strongly required.
29
30
31
32
33
34
35
36
37
38

351 **Acknowledgments**

352 SM is grateful to Naturalis Biodiversity Center for providing Martin Fellowships, which supported
353 fieldwork in Curaçao (2017) and Bonaire (2019). The fieldwork in Bonaire was also supported by a
354 grant from the WWF-Netherlands Biodiversity Fund to BWH. The staff of CARMABI Marine
355 Research Center at Curaçao is thanked for logistical support. We are grateful to STINAPA and DCNA
356 at Bonaire for assistance in the submission of the research proposal and the research permit.
357

358 **Figure Legends**

359 **Fig. 1** Sampling localities in the Caribbean Sea (Curaçao and Bonaire), Red Sea (Saudi Arabia), and
360 Indo-Pacific (Republic of the Maldives).
361
362
363
364
365

361
1
362
3
4
363
5
6
364
8
9
365
10
11
366
13
14
367
15
16
368
18
19
369
20
21
370
22
23
371
25
26
372
27
28
373
30
31
374
32
33
375
35
376
37
38
377
40
378
42
379
43
44
45
380
47
381
48
49
50
382
52
383
53
54
55
384
56
57
385
58
59
60
61
62
63
64
65

Fig. 2 *Halofolliculina* Ciliate Infection. **a** CCI affecting *Diploria labyrinthiformis*; **b** SEB affecting a coral of *Acropora muricata*; **c** close-up of halofolliculinids on a septum of *Eusmilia fastigiata*; **d** close-up of halofolliculinids on a colony of *Acropora muricata*. LC= live coral; DC= dead coral; the arrowheads indicate the cluster-like band of protozoans

Fig. 3 Various features of *Halofolliculina corallasia* and the peculiar single sculpture (S) of the lorica (Lor) in the three investigated areas: a-b) Indo-Pacific; c-d) Red Sea; e-f) Caribbean. Scale bars: 20 μm

Fig. 4 Mean values and SE of the neck diameter, neck length and the neck brim diameters of the *Halofolliculina* loricae affecting Indo-Pacific (Maldives and Red Sea) and Caribbean scleractinians. Mean values are expressed in μm .

Fig. 5 Scanning Electron Microscopy Images of Caribbean skeletal eroding pattern. **a** cluster of *Halofolliculina* ciliates on septae of *Diploria labyrinthiformis*; **b** close-up of loricae apparently eroding the host skeleton. **c** the white dashed line show the eroding pattern left by *Halofolliculina* ciliates on a colony of *Diploria labyrinthiformis*; **d** the round-shaped footprint of the loricae settlement observed on the same host; **e** apparently different eroding patterns associated to halofolliculinids; **f** black dashed line show slight footprints related to the presence of halofolliculinids. Scale bars: a 1 mm, b 0.5 mm, c-d 50 μm , e 10 μm , f 20 μm)

Fig. 6 Phylogenetic trees of *Halofolliculina* and relatives based on the ITS (a) and COI (b). Numbers at nodes show the Bayesian posterior probabilities and the ML bootstrapping values, respectively. ‘*’ indicates that a node is fully supported by both analyses. Halofolliculinids from different localities are

386 highlighted with different shades of yellow; other genera are highlighted in grey. RS: Red Sea; IN:
1
387 Indo-Pacific; CS: Caribbean Sea.
3

4
388
5

6

389 Tables

8

390 **Table S1.** Measurements of the diameter, length and width of both the neck and the ampulla of
10 *Halofolliculina corallasia*’ loricae
11

392 **Table S2.** Pairwise comparisons of genetic distance values (uncorrected *p*-distances in %) within and
393 between heterotrich genera and species based on ITS and COI.
14
394
15
395

16

396 References

17

397 Aeby GS, Ushijima B, Campbell JE, Jones S, Williams GJ, Meyer JL, Häse C, Paul VJ (2019)
20 Pathogenesis of a tissue loss disease affecting multiple species of corals along the Florida Reef Tract.

21
22 Front Mar Sci 6:678.
23

24

400 Antonius, A. (1999). *Halofolliculina corallasia*, a new coral-killing ciliate on Indo-Pacific reefs. Coral
401 Reefs 18: 300.
27
402
28
403

404 Antonius, A.A., Lipscomb, D. (2001). First protozoan coral-killer identified in the Indo-Pacific. Atoll
30 Res. Bull. 481:1–21
31
405
32
406

337 Beli E, Aglieri G, Strano F, Maggioni D, Telford MJ, Piraino S, Cameron CB (2018) The zoogeography
34 of extant rhabdopleurid hemichordates (Pterobranchia: Graptolithina), with a new species from the
35 Mediterranean Sea. Invertebr. Syst. 32: 100-110
36
407
37

398 Bourne DG, Garren M, Work TM, Rosenberg E, Smith GW, et al. (2009) Microbial disease and the
39 coral holobiont. Trends Microbiol. 17: 554–562.
40
41
413

414 Bourne, D. G., Ainsworth, T. D., Pollock, F. J., & Willis, B. L. (2015). Towards a better understanding
415 of white syndromes and their causes on Indo-Pacific coral reefs. Coral Reefs 34: 233-242.
44
416

417 Bruno JF, Selig ER (2007) Regional decline of coral cover in the Indo-Pacific: timing, extent, and
46 subregional comparisons. PLoS ONE 2: e711
47
48
489

490 Casamatta DA, Stani D, Gantar M, Richardson LL (2012) Characterization of *Roseofilum reptotaenium*
50 (Cyano bacteria, Oscillatoriales) gen. et sp. nov. isolated from Caribbean black band disease.
51 Phycologia 51:489-499
52
491
53

492 Castresana, J. (2000). Selection of conserved blocks from multiple alignments for their use in
54 phylogenetic analysis. Mol Biol Evol 17: 540-552.
55
493
56
494

495 Cróquer, A., Bastidas, C., Lipscomp, D., Rodríguez-Martínez, R. E., Jordan-Dahlgren, E., Guzman, H.
57 M. (2006a). First report of folliculinid ciliates affecting Caribbean scleractinian corals. Coral Reefs
58 25: 187-191.
59
60
61

62

63

64

65

430
431 Cróquer, A., Bastidas, C., Lipscomb, D. (2006b). Folliculinid ciliates: a new threat to Caribbean corals?
432 Dis. Aquat. Org 69: 75-78.
433
434 Darriba, D., Taboada, G. L., Doallo, R., Posada, D. (2012). jModelTest 2: more models, new heuristics
435 and parallel computing. Nature Methods 9:772
436
437 Dumontier, M., & Hogue, C. W. (2002). NBLAST: a cluster variant of BLAST for NxN comparisons.
438 BMC Bioinformatics 3: 13.
439
440 Fernandes, N. M., da Silva Paiva, T., da Silva-Neto, I. D., Schlegel, M., Schrago, C. G. (2016). Expanded
441 phylogenetic analyses of the class Heterotrichea (Ciliophora, Postciliodesmatophora) using five
442 molecular markers and morphological data. Mol. Phylogenet. Evol 95: 229-246.
443
444 Gardener T, Cote IM, Gill JA, Grant A, Watkinson AR (2003) Long-term region-wide declines in
445 Caribbean corals. Science 301: 958–960.
446
447 Hoeksema BW, Koh EGL (2009) Depauperation of the mushroom coral fauna (Fungiidae) of
448 Singapore (1860s–2006) in changing reef conditions. Raffles Bull Zool Suppl 22:91–101
449
450 Katoh, K., Standley, DM (2013). MAFFT multiple sequence alignment software version 7:
451 improvements in performance and usability. Mol Biol Evol 30: 772-780.
452
453 Katoh, K., Misawa, K., Kuma, K. I., Miyata, T (2002) MAFFT: a novel method for rapid multiple
454 sequence alignment based on fast Fourier transform. Nucleic Acids Res 30: 3059-3066.
455
456 Katz LA, DeBerardinis J, Hall MS, Kovner AM, Dunthorn M, Muse SV (2011) Heterogeneous rates of
457 molecular evolution among cryptic species of the ciliate morphospecies *Chilodonella uncinata*.
458 Journal of molecular evolution 73: 266-272.
459
460 Kumar S, Stecher, G, Li M, Knyaz C, Tamura K (2018) MEGA X: Molecular Evolutionary Genetics
461 Analysis across Computing Platforms. Mol Biol Evol 35: 1547-1549.
462
463 McManus, G. B., Xu, D., Costas, B. A., & Katz, L. A. (2010). Genetic identities of Cryptic species in
464 the *Strombidium stylifer/apolatum/oculatum* cluster, including a description of *Strombidium*
465 *rassoulzadegani* n. sp. Journal of eukaryotic microbiology 57: 369-378.
466
467 Meyer JL, Castellanos-Gell J, Aeby GS, Häse C, Ushijima B, Paul VJ (2019) Microbial community
468 shifts associated with the ongoing stony coral tissue loss disease outbreak on the Florida Reef Tract.
469 bioRxiv 626408
470
471 Miller MA, Holder MT, Vos R, Midford PE, Liebowitz T, Chan L, Warnow T (2009) The CIPRES
472 portals.
473
474 Montano S, Arrigoni R, Pica D, Maggioni D, Puce S. (2015). New insights into the symbiosis between
475 *Zanclaea* (Cnidaria, Hydrozoa) and scleractinians. Zool Scripta 44: 92-105
476
477 Page CA, Willis BL (2008) Epidemiology of skeletal eroding band on the Great Barrier Reef and the
478 role of injury in the initiation of this widespread coral disease. Coral Reefs 27: 257-272.
479
480

- 478 Page C A, Cróquer A, Bastidas C, Rodríguez S, Neale SJ, Weil E, Willis BL (2015) *Halofolliculina*
479 ciliate infections on corals (skeletal eroding disease). In: Woodley CM, Downs CA, Bruckner AW,
480 Porter JW, Galloway SB (eds.) Diseases of Coral, Wiley-Blackwell, Hoboken, pp 361-375.
481
- 482 Park, M. H., Jung, J. H., Jo, E., Park, K. M., Baek, Y. S., Kim, S. J., & Min, G. S. (2019). Utility of
483 mitochondrial CO1 sequences for species discrimination of Spirotrichea ciliates (Protozoa,
484 Ciliophora). Mitochondrial DNA Part A 30: 148-155.
485
- 486 Pollock FJ, Morris PJ, Willis BL, Bourne DG (2011) The urgent need for robust coral disease
487 diagnostics. PLoS Pathogens 7(10):e1002183
488
- 489 Primc-Habdija, B., Matoničkin, R. (2005). A new freshwater folliculinid (Ciliophora) from the karstic
490 region of Croatia. Eur J Protistol 41:, 37-43.
491
- 492 Rambaut A. (2012). Figtree v 1.4.0. <http://tree.bio.ed.ac.uk/software/figtree/>
493
- 494 Richardson LL (1998) Coral diseases: what is really known? Trends Ecol. Evol. 13: 438–443.
495
- 496 Riegl B, Antonius A (2003) *Halofolliculina* skeleton eroding band (SEB): a coral disease with
497 fossilization potential? Coral Reefs 22:48
498
- 499 Rodríguez S, Croquer A, Guzmán HM, Bastidas C (2009) A mechanism of transmission and factors
500 affecting coral susceptibility to *Halofolliculina* sp. infection. Coral reefs 28: 67-77.
501
- 502 Ronquist F, Teslenko M, van der Mark P, Ayres DL, Darling A, Höhna S, Larget B, Liu L, Suchard
503 MA, Huelsenbeck JP. 2012. MrBayes 3.2: efficient Bayesian phylogenetic inference and model
504 choice across a large model space. Syst. Biol. 61: 539-542.
505
- 506 Rosenberg E, Kelloff CA, Rohwer F (2007) Coral microbiology. Oceanography 20: 146–154.
507
- 508 Sutherland WJ, Clout M, Depledge M, Dicks LV, Dinsdale J, Entwistle AC, Fleishman E, Gibbons DW,
509 Keim B, Lickorish FA, Monk KA, Ockendon N, Peck LS, Pretty J, Rockström J, Spalding MD,
510 Tonneijck FH, Wintle BC (2015) A horizon scan of global conservation issues for 2015. Trends Ecol.
511 Evol. 30:17–24.
512
- 513 Sussman M, Bourne DG, Willis BL (2006) A single cyanobacterial ribotype is associated with both red
514 and black bands on diseased corals from Palau. Dis. Aquat. Organ. 69: 111-118
515
- 516 Stamatakis A (2006) RAxML-VI-HPC: maximum likelihood-based phylogenetic analyses with
517 thousands of taxa and mixed models. *Bioinformatics* 22: 2688-2690.
518
- 519 Stamatakis A (2014) RAxML version 8: a tool for phylogenetic analysis and post-analysis of large
520 phylogenies. *Bioinformatics* 30: 1312-1313.
521
- 522 Strüder-Kypke MC, Lynn DH (2010) Comparative analysis of the mitochondrial cytochrome c oxidase
523 subunit I (COI) gene in ciliates (Alveolata, Ciliophora) and evaluation of its suitability as a
524 biodiversity marker. *Syst Biodivers* 8: 131-148.
525
- 526 Sun P, Clamp JC, Xu D (2010) Analysis of the secondary structure of ITS transcripts in peritrich ciliates
527 (Ciliophora, Oligohymenophorea): Implications for structural evolution and phylogenetic
528 reconstruction. *Mol Phylogenet Evol* 56: 242–251

529
530
531
532
533
534
535
536
537
538
539
540
541
542
543
544
545
546
547
548
549
550
551
552
553
554
555
556
557
35
36
37
38
39
40
41
42
43
44
45
46
47
48
49
50
51
52
53
54
55
56
57
58
59
60
61
62
63
64
65

Sweet JM, Séré' GM (2015) Ciliate communities consistently associated with coral diseases. *J Sea Res* 113: 119-122

Talavera G, Castresana J (2007) Improvement of phylogenies after removing divergent and ambiguously aligned blocks from protein sequence alignments. *Syst Biol*, 56 564-577.

Weil E, Hooten, AJ (2008) Underwater cards for assessing coral health on Caribbean reefs. *Coral reefs targeted research and capacity building for management*, 24-pp.

Weil E, Rogers CS (2011) Coral reef diseases in the Atlantic-Caribbean. In: Dubinsky Z, Stambler N (eds.) *Coral Reefs: An Ecosystem in Transition* Springer, Dordrecht, Netherlands, pp 465–491

Willis BL, Page CA, Dindsdale EA (2004) Coral disease in the great barrier reef. In: Rosenberg E, Loya Y (eds) *Coral health and disease*. Springer, Berlin, pp 69–104

Winkler R, Antonius A, Abigail Renegar, D. (2004) The skeleton eroding band disease on coral reefs of Aqaba, Red Sea. *Mar Ecol* 25: 129-144.

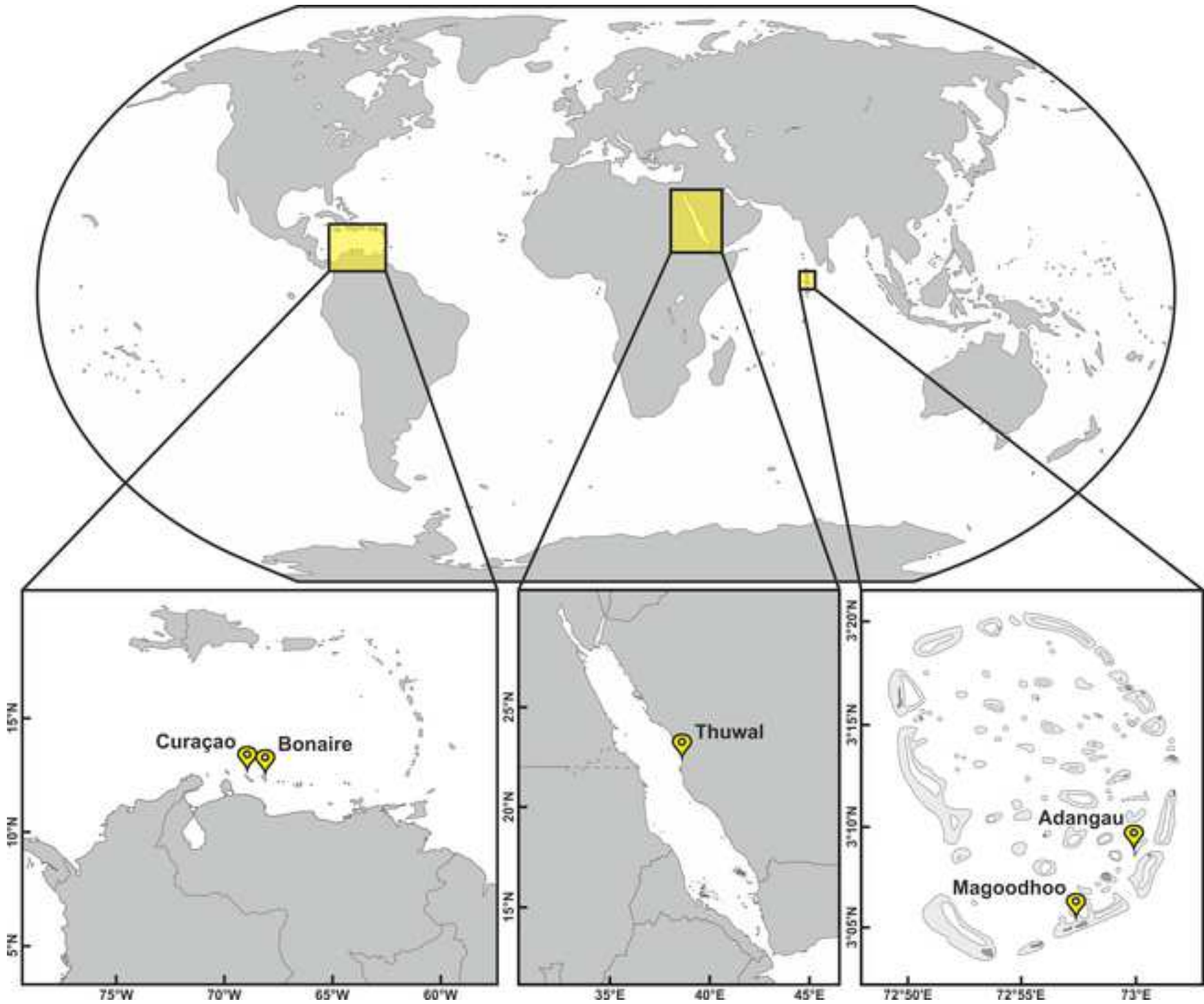
Woodley, Cheryl M.; Downs, Craig A.; Bruckner, Andrew W.; Porter, James W.; Galloway, Sylvia B. (2016). *Diseases of Coral*. Wiley-Blackwell, Hoboken,

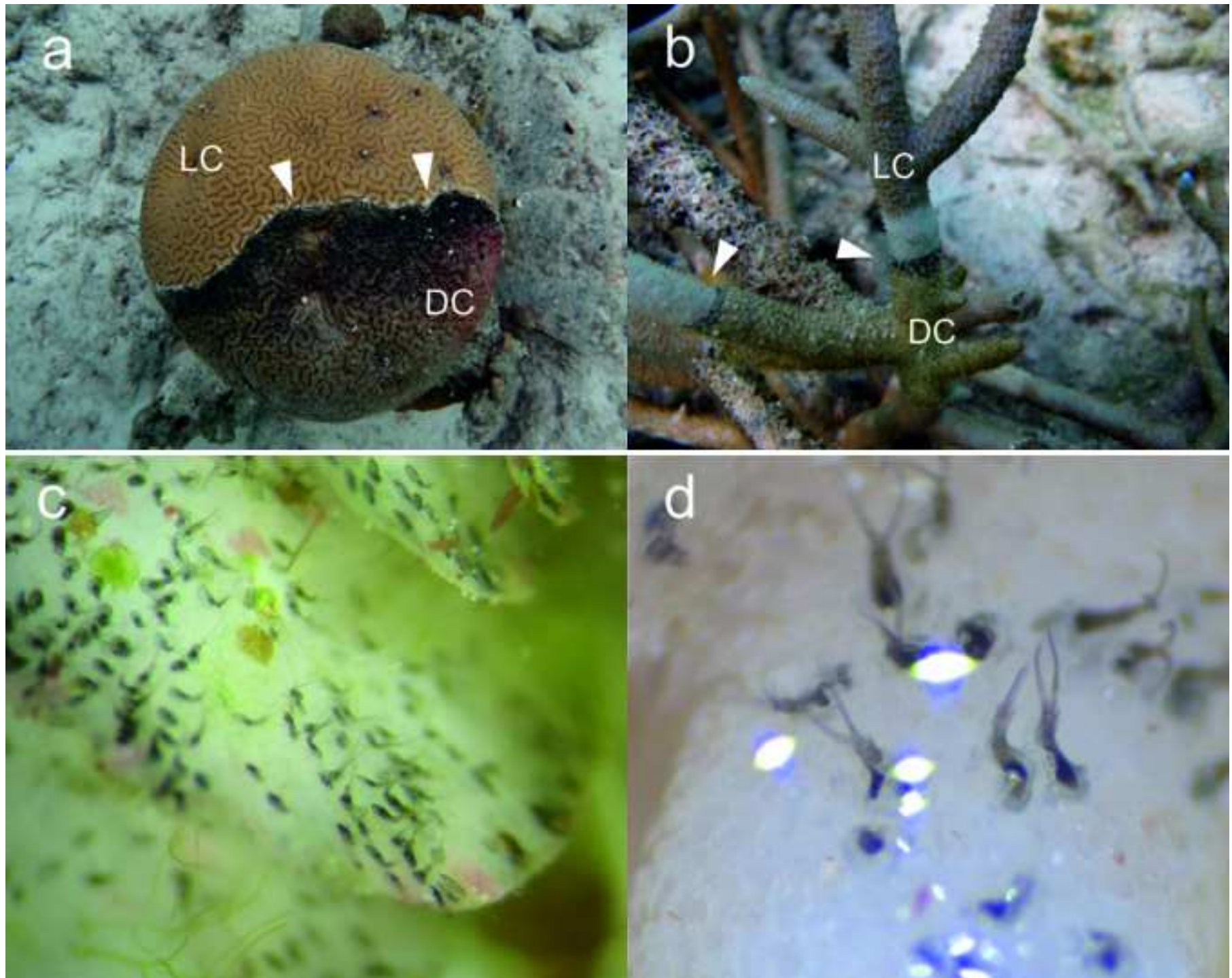
Work T, Meteyer C (2014) To understand coral disease, look at coral cells. *EcoHealth* 11: 610-618.

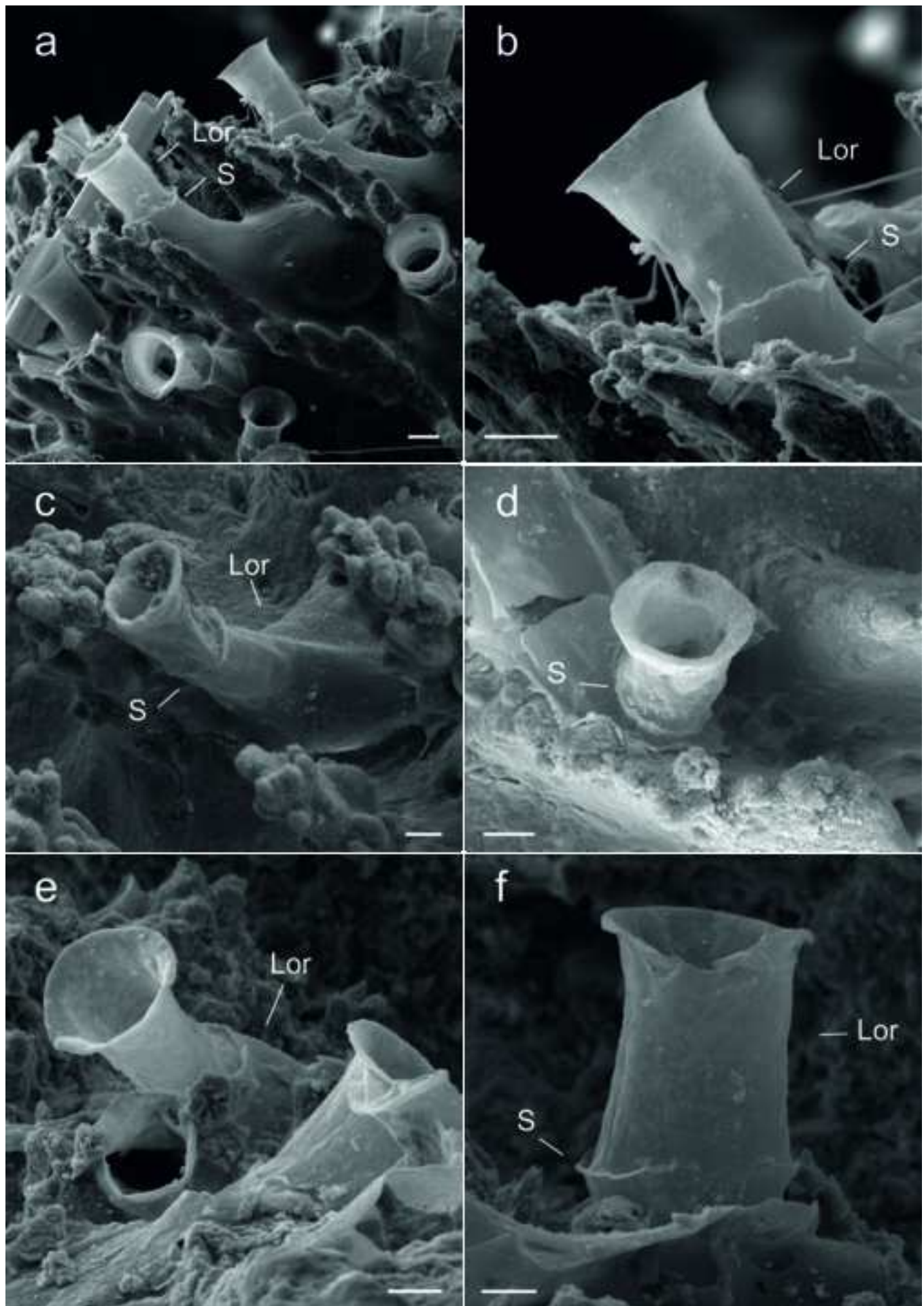
Yi Z, Song W (2011) Evolution of the order Urostylida (Protozoa, Ciliophora): new hypotheses based on multi-gene information and identification of localized incongruence. *PLoS ONE* 6, e17471.

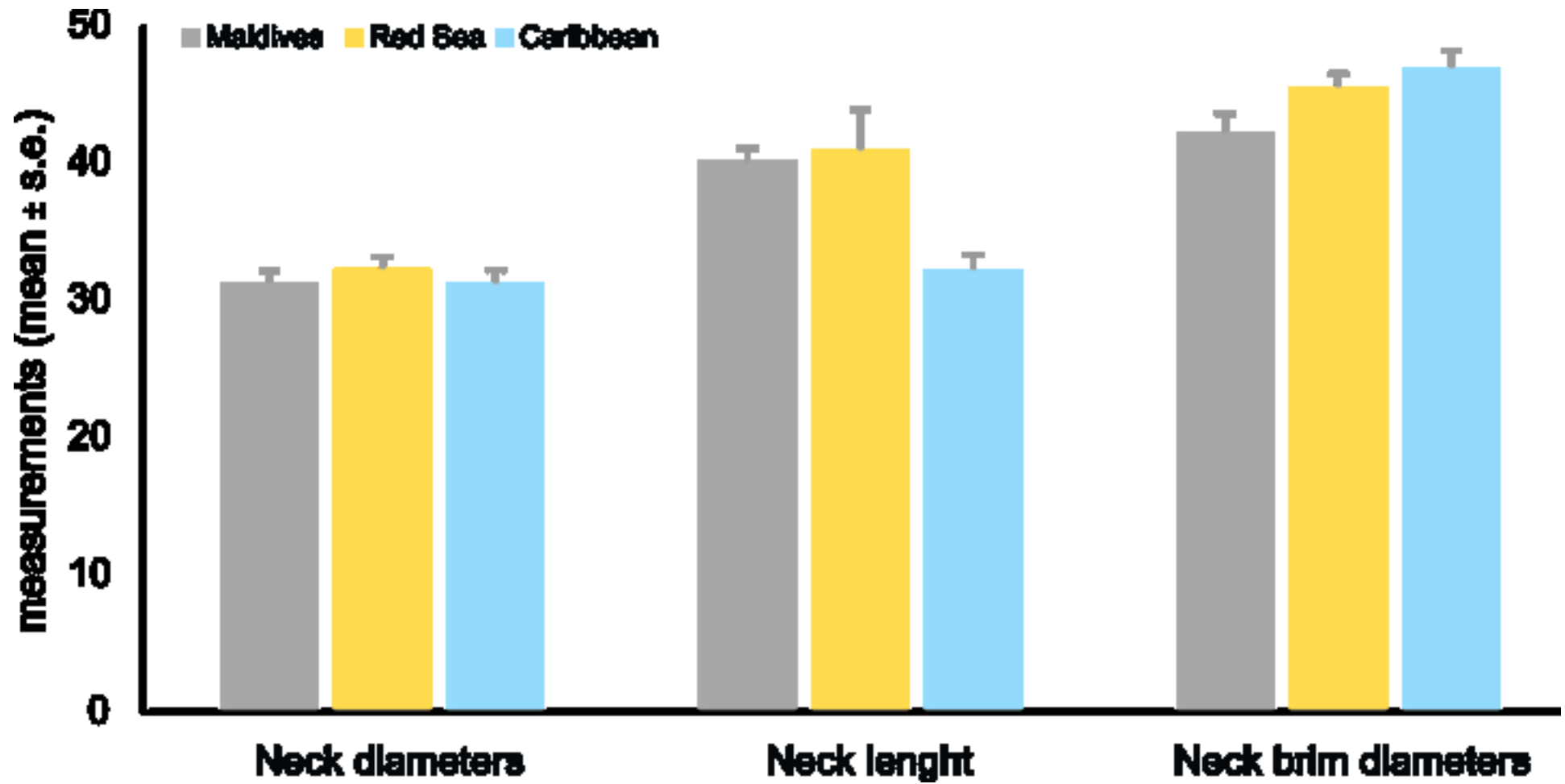
Zar JH (1999) *Biostatistical analysis*. Prentice-Hall, London

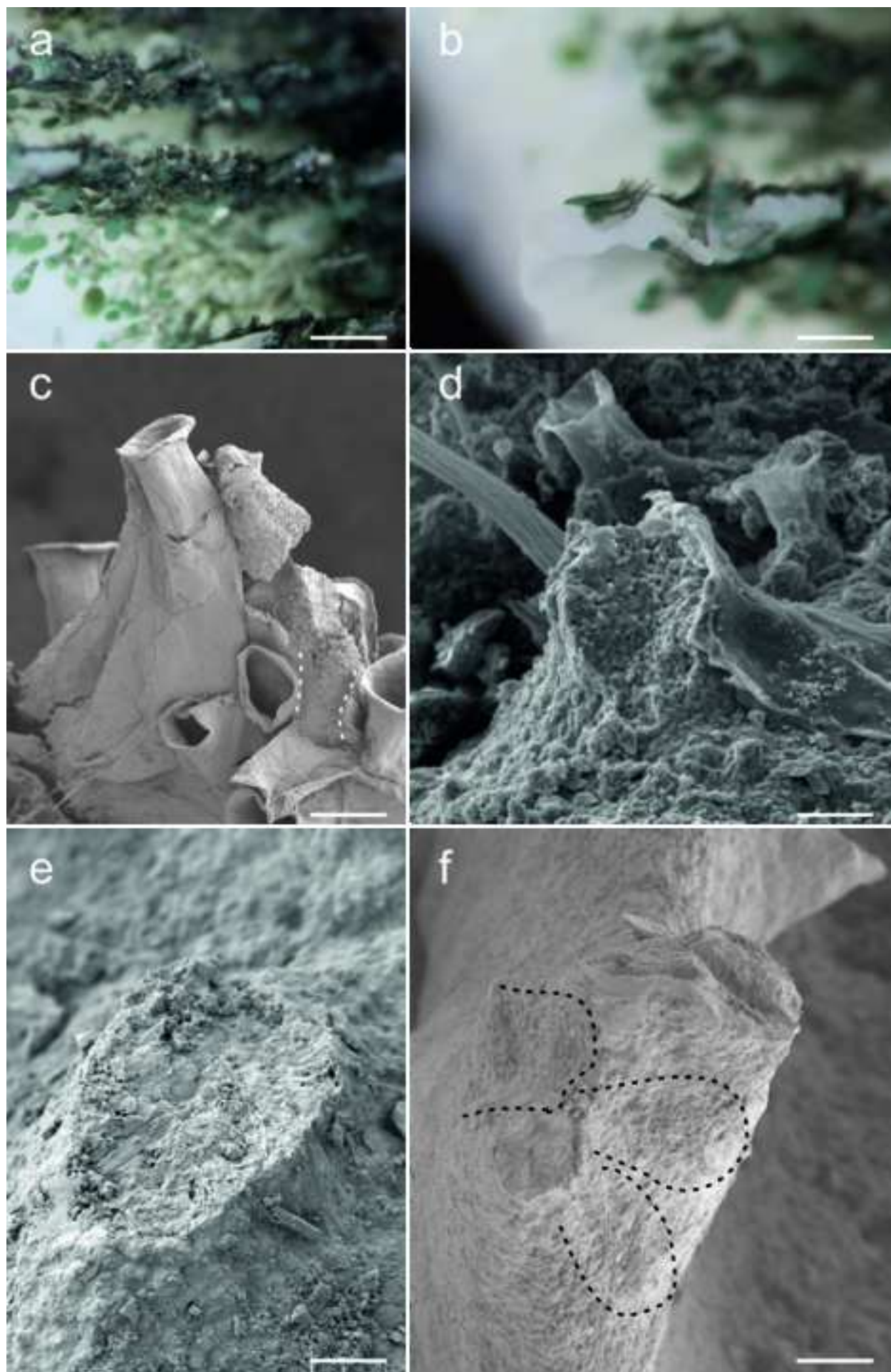
Figure 1

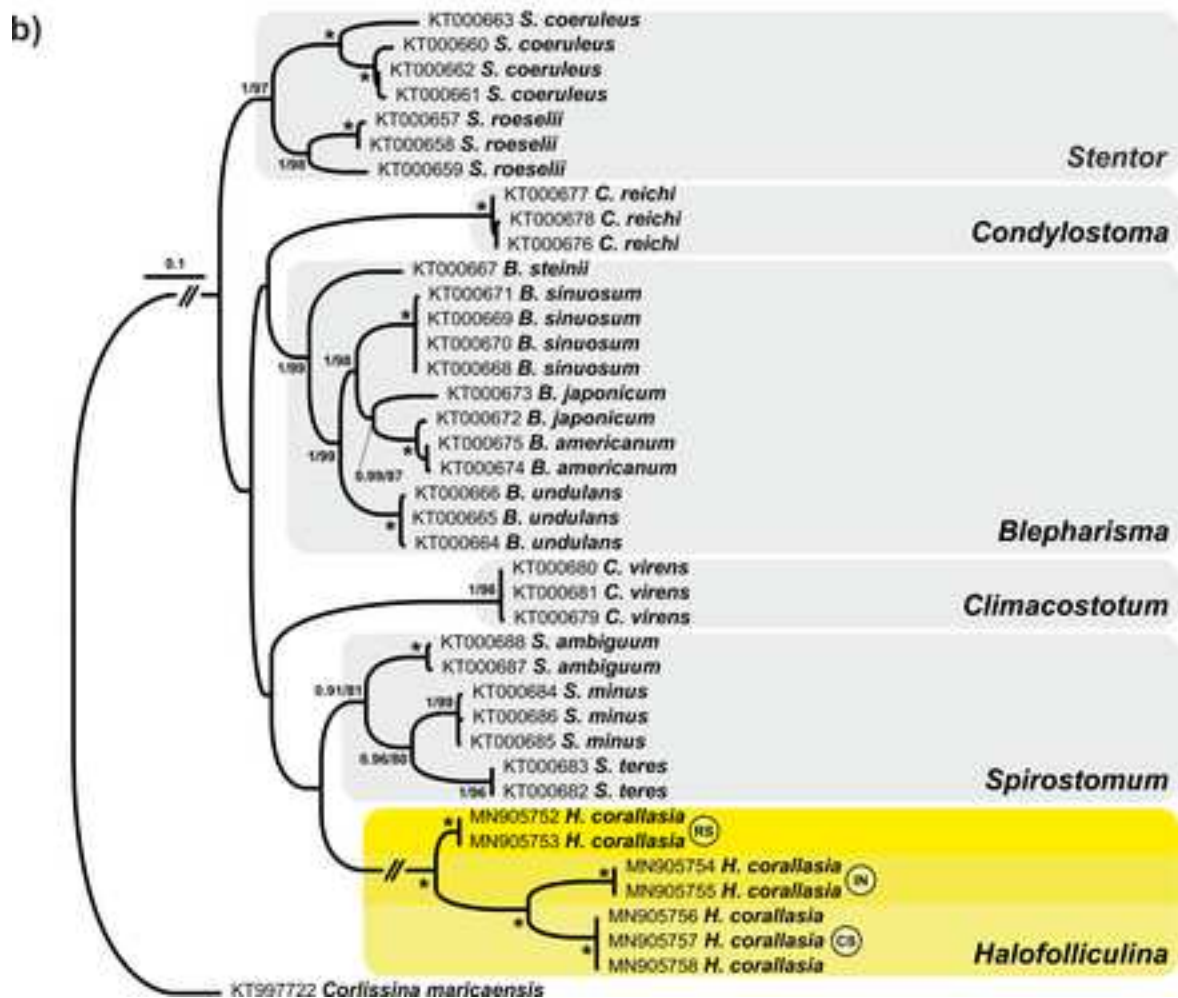
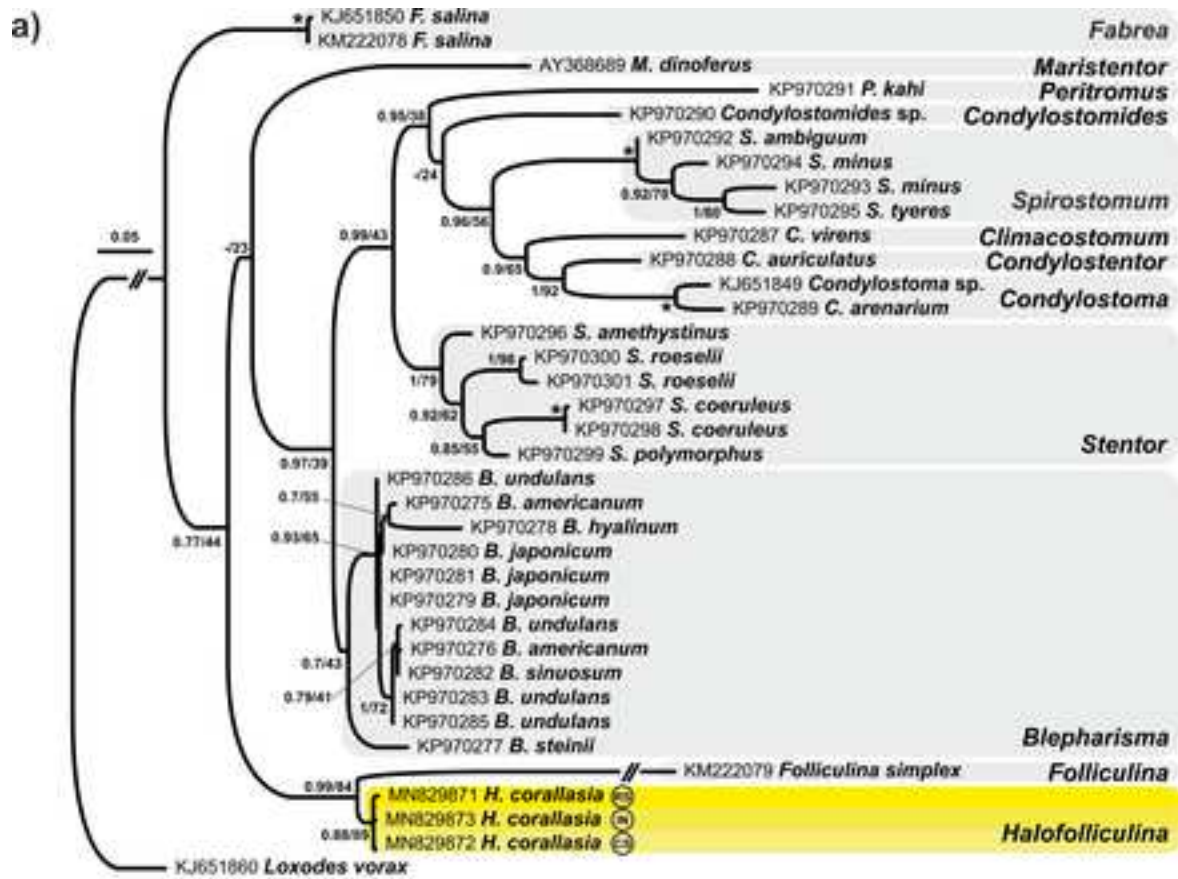


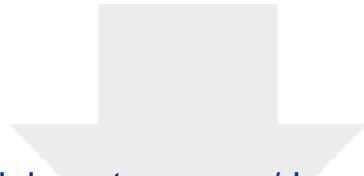








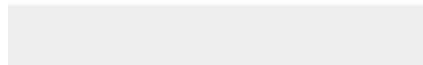


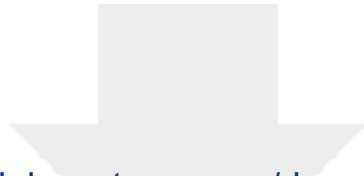


[Click here to access/download](#)

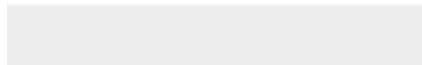
Supplementary Material

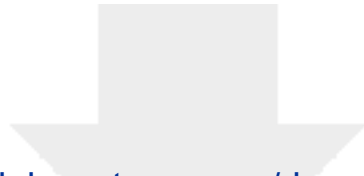
Revised_Table_S1_Montano et al..xlsx





Click here to access/download
Supplementary Material
Revised_Table_S2.xlsx





[Click here to access/download](#)

Supplementary Material

[Revised_Figure S1_Montano et al..docx](#)



1 **Morpho-molecular traits of Indo-Pacific and Caribbean *Halofolliculina* ciliate infections**

2

3 Simone Montano¹⁻² *, Davide Maggioni¹⁻², Giulia Liguori¹⁻², Roberto Arrigoni³⁻⁴⁻⁵, Michael L.
4 Berumen^{5,4}, Davide Seveso¹⁻², Paolo Galli¹⁻², Bert W. Hoeksema^{6,5,7,6}

5

6 ¹Department of Earth and Environmental Sciences (DISAT), University of Milan – Bicocca, Piazza
7 della Scienza, 20126, Milan, Italy.

8 ²MaRHE Center (Marine Research and High Education Center), Magoodhoo Island Faafu Atoll,
9 Republic of Maldives

10 ³Department of Biology and Evolution of Marine Organisms (BEOM), Stazione Zoologica Anton
11 Dohrn Napoli, Villa Comunale, 80121 Napoli, Italy,

Formatted: Font: (Default) Times New Roman, 12 pt

12 ^{3,4}European Commission, Joint Research Centre (JRC), Ispra, Italy

Formatted: Font: 16 pt

13 ^{5,4}Red Sea Research Center, Division of Biological and Environmental Science and Engineering, King
14 Abdullah University of Science and Technology, Thuwal 23955- 69-0-0, Saudi Arabia

15 ^{6,5}Taxonomy and Systematics Group, Naturalis Biodiversity Center, P.O. Box 9517, 2300 RA Leiden,
16 The Netherlands

17 ^{7,6}Groningen Institute for Evolutionary Life Sciences, University of Groningen, P.O. Box 11103, 9700
18 CC Groningen, The Netherlands

19

20 *Corresponding Author: Simone Montano, Department of Earth and Environmental Sciences (DISAT), University of
21 Milan – Bicocca, Piazza della Scienza, 20126, Milan, Italy Milano. E-mail: simone.montano@unimib.it; phone:
22 +390264483433

23

24 **Abstract**

25 Coral diseases are emerging as a major threat to coral reefs worldwide and although many of them
26 have been described, knowledge on their epizootiology is still limited. This is the case of the

27 *Halofolliculina* ciliate infections, recognized as the Skeletal Eroding Band (SEB) and Caribbean
28 Ciliate Infection (CCI), two diseases caused by ciliates belonging to the genus *Halofolliculina* (Class
29 Heterotrichea). Despite their similar macroscopic appearance, the two diseases are considered
30 different and their pathogens have been hypothesised to belong to different *Halofolliculina* species.
31 In this work, we analysed the morphology and genetic diversity of *Halofolliculina* ciliates collected
32 in the Caribbean Sea, Red Sea, and Indo-Pacific Ocean. Our analyses showed a strong macroscopic
33 similarity of the lesions and similar settlement patterns of the halofolliculinids from the collection
34 localities. In particular, the unique erosion patterns typical of the SEB were observed also in the
35 Caribbean corals. Fine-scale morphological and morphometric examinations revealed a common
36 phenotype in all analysed ciliates, unequivocally identified as *Halofolliculina corallasia*.
37 Phylogenetic analyses based on nuclear (ITS) and mitochondrial (COI) molecular markers
38 consistently found all samples as monophyletic. However, although the nuclear marker displayed an
39 extremely low intra-specific diversity, consistent with the morphological recognition of a single
40 species, the analyses based on COI showed a certain level of divergence between samples from
41 different localities. Genetic distances between localities fall within the intra-specific range found in
42 other heterotrich ciliates, but they may also suggest the presence of a *H. corallasia* species complex.
43 In conclusion, the presented morpho-molecular characterization of *Halofolliculina* reveals strong
44 similarities between the pathogens causing SEB and CCI and call for further detailed studies about
45 the distinction of these two coral diseases.

46

47 **Keywords:** ciliate, protozoan, syndrome, *Halofolliculina corallasia*, coral reefs, scleractinian
48 corals

49

50 **Introduction**

51

52 Coral reefs are declining worldwide, with an estimated coral cover loss of 50% in the Indo-Pacific
53 and 80% in the Caribbean over the last 30 years (Gardener et al. 2003; Bruno and Selig 2007; Pollock
54 et al. 2011). The causes of this decline are multiple and complex, with coral diseases emerging as one
55 of the most affecting threats (Rosenberg et al. 2007; Bourne et al. 2009; Sutherland et al. 2015).

56 Currently, it is not clear how many coral diseases exist globally, and a certain level of confusion
57 emerges from the incomplete information reported in the literature (Willis et al. 2004). Indeed, despite
58 their negative impact, the majority of coral diseases remain a mystery, as a result of the limited
59 analytic methods, the poor knowledge of the putative pathogens and the consequent deficiency of
60 epizootiological data (Work and Meteyer 2014; Bourne et al. 2015). One of the most dramatic and
61 recent examples is the Stony Coral Tissue Loss Disease (SCTLD), which has been affecting various
62 coral species along the Florida Reef Tract since 2014 (Aeby et al. 2019). Although its effect is
63 unprecedented, all the efforts carried out by research have so far not been successful in discovering
64 its causative agents (Meyer et al. 2019). The lack of specific and accurate diagnostic tools coupled
65 with difficulties encountered in the study of bacteria-based diseases resulted also in ambiguous
66 classifications of coral diseases that remain largely open to interpretation (Pollock et al. 2011). The
67 shortage of multidisciplinary approaches to describe coral lesions and to identify morphologically
68 and molecularly the pathogens have led to recognize a high number of possibly different diseases,
69 which often share similar gross morphology of the lesions, as for the Indo-Pacific White Syndromes
70 (Bourne et al. 2015). Furthermore, in some cases diseases were named differently, even if caused by
71 the same putative pathogens. This is the case of the Black Band Disease (BBD) and the Red Band
72 Disease (RBD) of Palau, in which the filamentous cyanobacteria forming red and black bands were
73 molecularly identified as belonging to a single ribotype discovered to be caused by the same
74 pathogenic cyanobacteria only after their isolation, culturing and sequencing (Sussman et al. 2006).

75 Moreover, this scenario is further complicated by the existence of coral diseases caused by a
76 consortium of pathogens that may slightly differ among geographic areas. Therefore, the BBD,
77 recognized as a worldwide distributed disease caused by a consortium of microorganism dominated

78 by a cyanobacterial component, may differ in its predominant portion between the Caribbean and
79 Indo-Pacific (Casamatta et al. 2012).

80 The Skeletal Eroding Band (SEB) is one of the first coral diseases detected and described from ~~an~~the
81 Indo-Pacific coral reefs (Antonius 1999). It is caused by the folliculinid ciliate *Halofolliculina*
82 *corallasia* Antonius and Lipscomb, 2001 (Class Heterotrichea; Order Heterotrichida), which not only
83 attacks the soft tissues of corals but also damages their skeleton (Antonius and Lipscomb 2001; Riegl
84 and Antonius 2003; Page and Willis 2008). In *H. corallasia*, the lorica (sac-like housing) has a
85 rounded posterior and a cylindrical neck that angles up from the surface at about 45°, and it has an
86 average length and width of 220 µm and 95 µm, respectively. They are ~~deeply embedded in~~settled
87 on the coral skeleton, usually following the rim of the corallites, and in most cases only the neck rises
88 above the coral surface. The disease manifests as a dark-grey band 1–10 cm thick, located at the
89 interface between recently exposed skeleton and apparently healthy coral tissue. The SEB has been
90 recorded affecting 82 scleractinian species on various Indo-Pacific and Red Sea coral reefs, with the
91 most affected taxa being branching species of *Acropora* and *Pocillopora* (Page et al. 2015).
92 According to these data, the SEB shows the widest host range of any coral disease recorded to date,
93 reaching the top on the list of harmful coral syndromes (reviewed by Page and Willis 2008).
94 In 2004-2005, a similar ciliate infection was reported from 25 out of about 60 Caribbean coral species
95 (Cróquer et al. 2006a; Page et al. 2015), in which the infection appeared as a dark band located
96 between healthy tissue and bare skeleton, showing, on closer inspection, the characteristic spotted
97 appearance of the clustering ciliates (Cróquer et al. 2006a). The general morphology of the Caribbean
98 ciliate is very similar to that of *Halofolliculina corallasia* from the Indo-Pacific (Cróquer et al.,
99 2006b, Rodriguez et al. 2009). Both ciliates have a free-living phase that moves toward living tissues,
100 penetrates them and attaches itself, and a sessile form settled in a lorica, with the cell body attached
101 at its pointed posterior end, showing two conspicuous pericytostomial wings bearing feeding cilia
102 (Antonius, 1999; Antonius and Lipscomb, 2001; Cróquer et al., 2006b).

103 Despite a similar fine-scale morphology among *Halofolliculina* ciliates affecting Indo- Pacific and
104 Caribbean corals, the skeletal erosion is often associated with SEB, but not with the Caribbean ciliate
105 infections to date (Page et al. 2015). However, no information is present in the literature about the
106 apparent no-eroding pattern of ciliate affecting Caribbean corals, leaving space for additional in-depth
107 studies.

108 Initially, it was proposed that these ciliates might have recently invaded the Caribbean from the Indo-
109 Pacific region (Cróquer et al. 2006b), but then the authors stated that the Caribbean and Indo-Pacific
110 ciliates are different species, based on unpublished data (Cróquer et al. 2006a). Despite the Caribbean
111 pathogen is still to be formally characterised and described at species level, researchers suggested the
112 name Caribbean Ciliate Infections (CCI) to indicate the presumed new disease, due to the apparent
113 differences in aetiology (Weil and Hooten 2008; Rodríguez et al. 2009; Weil and Rogers 2011). By
114 contrast, it has also been reported by Sweet and Serè (2016) that SEB and CCI are caused by the same
115 pathogen, despite an absence of evidence to support this conclusion.

116 Therefore, the goal of this study is to improve the knowledge concerning the *Halofolliculina* Ciliate
117 Infections (*sensu* Page et al. 2015) by investigating the aetiology of SEB and CCI through a morpho-
118 molecular approach, in order to assess and confirm possible taxonomic affinities between the
119 *Halofolliculina* species.

120

121 **Material and methods**

122 Sampling was conducted between June 2017 and October 2019 in three geographic areas, including
123 the Indian Ocean (Republic of the Maldives), the Red Sea (Saudi Arabia) and the Caribbean Sea
124 (Curaçao and Bonaire) (Fig. 1).

125 The presence of the *Halofolliculina* Ciliate Infection was qualitatively recorded both by snorkeling
126 and SCUBA diving through a roving technique (Hoeksema and Koh, 2009). A dive of
127 approximately one hour was carried out at each sampling locality, starting from a maximum depth
128 of 10–25 m and moving towards shallower waters. In each locality, two to four small diseased coral

129 fragments were taken with a hammer and chisel from colonies showing the characteristic band.
130 Underwater photographs were taken using a Canon GX7 Mark II camera in a Fantasea GX7 II
131 underwater housing. Diseased coral colonies used in the study were chosen randomly (depending on
132 their abundance) and include *Pocillopora* spp. and *Porites lutea* in the Indo-Pacific and the Red Sea,
133 and *Eusmilia fastigiata* and *Diploria labyrinthiformis* in the Caribbean Sea. After a preliminary
134 observation, samples were fixed in formalin 6% and ethanol 99%, for further morphological and
135 molecular analyses, respectively.

136 Halofolliculinid protozoans were initially observed *in vivo* with a Leica EZ4 D stereomicroscope to
137 examine the protozoan aggregations and to search for possible macroscopic differences, such as a
138 different colouration and the shape of the lorica. Then, single individuals were detached from the
139 coral skeleton using needles, precision forceps and micropipettes and placed on a glass slide to
140 observe their morphology at higher magnification under a Zeiss Axioskop 40 microscope.
141 Subsequently, ten coral fragments belonging to the four genera (*Diploria*, *Eusmilia*, *Pocillopora*,
142 *Porites*) were observed using both the Tescan Vega TS 5136 XM scanning electron microscope,
143 operating at beam energies of 20kV, and the Zeiss Gemini SEM500 scanning electron microscope
144 operating at beam energies of 5kV. About 30 loricae were randomly chosen for each coral fragment
145 to take measurements of the diameter, length and width of both the neck and the ampulla, according
146 to Antonius and Lipscomb (2001) and Primc-Habdija et al. (2005) (Fig. S1). Measurements were
147 recorded using the Scanning Electron Microscope measuring software SmartSEM (ZEISS,
148 Oberkochen, Germany) with maximum resolution of 1 nm. Additionally, a preliminary
149 characterisation of the skeletal erosion caused by the CCI has also been carried out through SEM
150 imaging.

151 The morphometric measurements were tested for normality distribution with a Shapiro-Wilk test of
152 normality. One-way analyses of variance (ANOVA) were performed to test for differences in the
153 neck diameter between localities, whereas differences in the length of the neck and diameter of the
154 neck brim were tested using a non-parametric Kruskal-Wallis test, since the data were not normally

155 distributed (Zar 1999). Ampullae length and width of *Halofolliculina* loricae were analysed by
156 descriptive statistics due the few observations obtained. Statistical analyses were performed using
157 SPSS ver. 24 (IBM, New York). All data are presented as mean \pm standard error (SE), unless
158 otherwise stated.

159

160 ***Molecular analyses***

161 The genomic DNA was extracted following a protocol already successfully used for different taxa
162 (Montano et al. 2015; Beli et al. 2018). Two molecular markers were amplified, namely a portion of
163 the nuclear ITS (~400 bp) and the mitochondrial COI gene (~600 bp), following the protocols
164 described in Fernandes et al. (2016) and Strüder-Kypke and Lynn (2010), respectively. These two
165 DNA regions were chosen because they are generally considered reliable markers to infer ciliate
166 phylogeny (e.g. Sun et al. 2010; Yi and Song 2011; Fernandes et al. 2016) and because they show
167 different substitution rates, with the COI being the more variable marker and having been already
168 used to assess ciliates intra-specific variability (e.g. Gentekaki and Lynn 2009; Strüder-Kypke and
169 Lynn 2010). The amplicons were purified and sequenced in both forward and reverse directions using
170 a DNA Analyser 3730xl (Applied Biosystems, California, USA). The obtained sequences were
171 imported, assembled, and visually checked into Geneious R7. For each molecular marker, a dataset
172 was assembled adding sequences belonging to halofolliculind relatives downloaded from GenBank.
173 Sequences from two karyorelictid species (*Corlissina maricaensis*, *Loxodes vorax*) were also
174 included as outgroups. Sequences were aligned using the E-INS-i option in MAFFT 7.402 (Kato
175 and Standley, 2013), and were then run through Gblocks (Castresana 2000; Talavera and Castresana,
176 2007) to remove low quality and ambiguously aligned positions. Phylogenetic analyses were
177 performed using Bayesian Inference (BI) and Maximum Likelihood (ML). JmodelTest2 2.1.6
178 (Darriba et al., 2012) was run to find the proper molecular models, and the best-fitting model selected
179 for both datasets was GTR+G, as suggested by the Aikaike Information Criterion (AIC). BI analyses
180 were performed using MrBayes 3.2.6 (Ronquist et al., 2012): four parallel Markov Chain Monte Carlo

181 runs (MCMC) were run for 10^7 generations, trees were sampled every 1000th generation, and burn-
182 in was set to 25%. ML analyses were performed with RAxML v8.2.10 (Stamatakis, 2006, 2014)
183 using 1000 bootstrap replicates. Resulting trees were displayed and edited using FigTree 1.4.0
184 (Rambaut, 2012) and CorelDraw X7 (Corel Corporation, Ottawa, Canada). Genetic distances
185 (uncorrected *p*-distances, 1000 bootstrap) among and within heterotrich lineages were obtained for
186 both molecular markers using MEGA-X (Kumar et al., 2018). The obtained sequences were deposited
187 in GenBank (accession numbers: [ITS: MN829871-MN829873](#); [COI: MN905752-](#)
188 [MN905758](#)~~XX000000-XX000000~~) with relative sample codes and sampling sites.
189

190 **Results**

191 *Morphological results*

192 Our ecological surveys reveal the presence of *Halofolliculina* Ciliate Infections diseases in all three
193 investigated areas. First examinations revealed clusters of protozoans placed on coral surface between
194 recently exposed skeleton and apparently healthy coral tissues, forming dense bands characterised by
195 a dark green, almost black, colour pattern in diseased corals from both the Caribbean and the Indo-
196 Pacific (Fig. 2 a-b). In all samples, protozoans matched the description of *Halofolliculina corallasia*
197 provided by Antonius and Lipscomb (2000). The body was covered by rows of cilia and showed the
198 two characteristic bifurcate pericystomial wings bearing the oral polykinetids (Fig. 2 c-d).

199 To better visualize the morphology of the loricae and to confirm their identification, a total number
200 of 109 loricae (24 on *Porites lutea*, 29 on *Eusmilia fastigiata*, 10 on *Diploria labyrinthiformis*, 35 on
201 *Pocillopora damicornis*, and 11 on *Pocillopora verrucosa*) were examined using the SEM. All the
202 loricae had a rounded posterior and a cylindrical neck with a single sculpture line circumscribing it
203 (Fig. 3). Furthermore, no significative differences in the overall distribution, settlement patterns and
204 general size of the loricae have been observed between the coral genera and localities investigated.

205 In general, the mean ampulla length (*l*) and width (*w*) were higher in the Caribbean samples (*l*= 146.4
206 ± 4.3 μm; *w*= 83.3 ± 6.2 μm) compared to the Maldivian specimens (*l*= 112.7 ± 4.1 μm; *w*= 62.1 ±

207 4.7 μm) and the Red Sea specimens ($l= 54.3 \mu\text{m}$; $w= 51.1 \mu\text{m}$). Regarding the length of the neck,
208 mean values of $40.1 \pm 1.0 \mu\text{m}$ and $40.9 \pm 3.1 \mu\text{m}$ were observed in the Maldivian and Red Sea
209 specimens, respectively, whereas a mean value of $32.2 \pm 1.1 \mu\text{m}$ was observed for the Caribbean
210 ciliates. Furthermore, similar values were found for the neck diameter, with Maldivian, Red Sea and
211 Caribbean ciliates showing mean values of $31.25 \pm 0.9 \mu\text{m}$, $32.28 \pm 0.9 \mu\text{m}$ and $31.20 \pm 1.0 \mu\text{m}$,
212 respectively (Fig. 4).

213 According to the parametric and non-parametric tests performed, the neck diameters and neck lengths
214 were not statistically different between the three geographic areas (neck diameters: ANOVA
215 $F_{2,90}=0.406$, $p=0.668$; neck length: Kruskal-Wallis $H=6.06$ $p = 0.051$). In contrast, a significant
216 difference was observed for the neck brim diameter between the three geographic areas, with the
217 Maldivian specimens showing a mean value of $42.2 \pm 1.4 \mu\text{m}$, the Red Sea of $45.5 \pm 1.0 \mu\text{m}$ and the
218 Caribbean of $46.9 \pm 1.3 \mu\text{m}$ (Kruskal-Wallis $H=8.38$ $p = 0.015$). Maximum and minimum
219 morphometric data of the loricae from each of the geographic areas are summarized in Table S1.

220 In addition, peculiar micro-alterations have been identified on the surface of the skeleton of the
221 Caribbean scleractinian genera at locations where *Halofolliculina* ciliates were present (Fig. 5a). The
222 ciliates appear to modify the growth pattern of the host coral, apparently eroding part of the skeleton
223 and producing a round-shaped trace where the ciliates were located (Fig. 5 b-c). This results in distinct
224 footprints or marks on the coral surface attributable to the protozoans settlement. The shape of the
225 footprint appears cylindrical, although generally not regular, with a diameter ranging from about 50
226 μm in width to 95 μm in length (Fig. 5d). In some coral colonies a less evident eroded pattern,
227 ascribable to the presence of the loricae on the skeleton was also observed (Fig. 5 e-f).

228

229 ***Molecular results***

230 The total alignments of the ITS and COI datasets after the Gblocks treatment were 455 and 688 bp
231 long, and consisted in 36 and 40 sequences, respectively. BI and ML analyses resulted in almost
232 identical phylogenetic trees, and therefore only the ML topologies are shown in Fig. 4, with nodal

233 supports indicated as Bayesian posterior probabilities (BPP) and bootstrap supports (BS). The ITS
234 tree (Fig. 6a) shows an overall moderate to good nodal support for the Bayesian analysis, whereas
235 the ML analysis resulted in less supported relationships. All included genera are monophyletic, but a
236 few species are not. The *Halofolliculina* sequences obtained from different localities form a
237 monophyletic clade (BPP = 0.88, BS = 89), sister to *Folliculina simplex* (BPP = 0.99, BS = 84), the
238 only other folliculinid included in the analysis. The evolutionary relationships represented in the COI
239 tree (Fig. 6b) show higher support values for both BI and ML analyses at genus and species level, but
240 deeper nodes are generally less supported. However, all genera and species included in the analysis
241 are monophyletic, including the *Halofolliculina* clade (BPP = 1, BS = 100). In comparison to the ITS
242 analyses, the halofolliculinids collected from different localities show a higher diversification, and
243 three geography-related, fully supported lineages can be identified.

244 Genetic distances calculated between heterotrich species and genera are generally high, especially for
245 the COI dataset (Table S2). The average distances between genera and species for the COI dataset
246 are 39.9% (28.5 - 58.5%) and 32% (8.6 - 59.1%), respectively, with *Halofolliculina* showing the
247 highest distances towards all other sequences (Table S2). Distances between genera and species in
248 the ITS dataset are lower, being 21.8% (13.1 - 38.7 %) and 18% (0.4 - 39.4%), respectively (Table
249 S2). The intra-specific distances are higher for the COI dataset, ranging from 0 to 14%, whereas they
250 are lower for the ITS dataset (0.1 - 7.3%) (Table S2). Regarding the *Halofolliculina* sequences, intra-
251 [clade-genus](#) distances are moderately high for the COI ($14 \pm 0.9\%$), but very low for the ITS ($0.5 \pm$
252 0.4). [The genetic distances between *Halofolliculina* samples from the three localities are high, ranging](#)
253 [from 18.6 to 21.1% \(Table S2\).](#)

255 Discussion

256 The present work reveals the relationship between *Halofolliculina* ciliate infections known as Skeletal
257 Eroding Band in the Indo-Pacific and as Caribbean Ciliate Infection in the Caribbean, by the

258 application for the first time, of an integrative, morphological-molecular approach. Coral lesions and
259 protozoans in the three geographic areas showed the same macroscopic appearance.

260 In all investigated affected coral species, halofolliculinid infestations manifested themselves as areas
261 of tissue loss and bare skeleton covered by loricae. *Halofolliculina* ciliates settle in clusters following
262 the rim of the corallites and represent dark dots, giving the skeleton a scattered appearance. When in
263 high densities they form a thick band (1-10 cm), usually black or dark green in colour, between
264 recently exposed skeleton and dead tissue. They can also form more speckled bands when in low
265 density and be more light green in colour. Thus, the *in vivo* observation of halofolliculinids confirmed
266 the previous information reported for the Skeletal Eroding Band disease (Antonius and Lipscomb
267 2000; Winkler et al. 2004; Page and Willis 2008) and the Caribbean Ciliate Infection (Croquer et al.
268 2006a). In particular, the analysis of the main features of the protozoans' body and lorica matched
269 with the description of *Halofolliculina corallasia* provided by Antonius and Lipscomb (2000) for all
270 specimens analyzed. Moreover, a detailed analysis of the skeleton revealed an erosion on Caribbean
271 diseased corals, suggesting for the first time settlement patterns similar to those of Indo-Pacific SEB-
272 affected corals. In particular, slightly eroded marks related to the presence of *Halofolliculina* loricae
273 have been observed on the Caribbean skeletons, revealing that the ciliate may use the same
274 mechanisms as in Indo-Pacific SEB-causing ciliates. Indeed, the Caribbean *Halofolliculina* ciliates
275 seems to manifest an apparently chemical activity by leaving "sack-shaped" borings or an
276 "honeycomb" pattern while attach their bodies on the coral skeleton as already reported for the Indo-
277 Pacific counterpart (Riegl and Antonius 2003). The footprints were consistent with the position and
278 size of the loricae of *H. corallasia*, although apparently different erosion degree within the same
279 samples or host has been detected. If ~~it~~[this](#) is related to the time they remain attached to the [coral](#)
280 ~~host~~[corals](#) or if some other unknown factors are involved needs to be elucidated in future research.

281 The main character used to distinguish *H. corallasia* from its congeners is the presence of a single
282 sculpture line circumscribing the neck of the lorica (Antonius and Lipscomb 2000; Page et al. 2015).

283 The single line was evident and easily detectable in all examined protozoans from the Indo-Pacific,

284 Red Sea, and the Caribbean. In addition, all the obtained measures fall within the ranges estimated
285 for *H. corallasia* in its first description (Antonius and Lipscomb 2000). Statistical analyses revealed
286 no significant differences in the neck diameter and length, supporting the fine-scale morphological
287 similarities of halofolliculinids from the Caribbean and Indo-Pacific. Although a statistical difference
288 was found in the neck brim diameters, we believe this morphological character needs further
289 investigation since, in a few cases, loricae were distorted mainly due to the conservation of the sample
290 and to the great variability in the extensibility of the lorica (Primc-Habdija and Matoničkin, 2005),
291 and this may have introduced a bias in the measurements. Therefore, all individuals have
292 morphologically been identified as *H. corallasia*, and protozoans found in the Caribbean appeared to
293 be identical to those causing the SEB in the Indo-Pacific and Red Sea.

294 Overall, the understanding of the genetic relationships among ciliates is complicated by the
295 incomplete knowledge of their diversity (Strüder-Kypke and Lynn, 2010). Indeed, ciliated protozoans
296 are largely underrepresented in current biodiversity estimates for many reasons, such as their small
297 size and the difficulty in their isolation and culture (Kher et al., 2011). In line with this gap of
298 knowledge, no genetic information on *H. corallasia* and the whole genus *Halofolliculina* has been
299 presented so far in the literature and no sequences have been deposited in [GenBank public databases](#).
300 Consequently, the DNA sequences herein obtained are the first molecular data for the entire
301 *Halofolliculina* genus and represent a starting point for future genetic evaluations of the species and
302 related taxa.

303 The molecular results partially diverge from the morphological characterization, finding relevant
304 differences between protozoans from different localities. Although both nuclear and mitochondrial
305 molecular markers revealed the monophyly of all *H. corallasia* individuals sequenced in this work,
306 ITS and COI markers showed variable levels of variation in protozoans from different localities. The
307 *H. corallasia* intra-specific genetic distance based on the ITS dataset was extremely low, whereas
308 that based on COI was higher. [Moreover, genetic distances between *Halofolliculina* from the three](#)
309 [different localities were remarkably high](#). These results agree with previous works on ciliate genetic

310 diversity, in which COI showed a much higher diversification than the ITS region (Gentekaki and
311 Lynn 2009; Fernandes et al. 2016).

312 According to these molecular results, we may hypothesize two main opposite scenarios. Firstly, we
313 may be dealing with a single species with a circumtropical distribution. Indeed, the high ~~between-~~
314 ~~localities~~intra-*Halofolliculina* genetic distances observed for the COI fall within the range of intra-
315 specific distances found for other heterotrich species. The inter-specific divergence is generally much
316 higher in ciliates than in animals and the genetic distance thresholds used for species delimitation
317 differ greatly among ciliate taxa, being for instance around 1% for *Tetrahymena* spp. and 18% for
318 *Carchesium* spp., based on the COI (Gentekaki and Lynn, 2009; Kher et al., 2011). These data suggest
319 that evolution rates can be extremely high in ciliates, and that their intra-specific genetic diversity
320 can vary largely among taxa and could be taxon-specific (Gentekaki & Lynn, 2009; Strüder-Kypke
321 and Lynn, 2010). Researchers have suggested that a high ciliate genetic diversity can depend on
322 several factors, such as a strong gene flow and the ability of the dispersal phase of these
323 microorganisms to reach large distances (Gentekaki and Lynn, 2009). It is also assumed that, in
324 population of ciliates highly isolated from each other, a positive correlation exists between their
325 genetic divergence and the geographic distance, such as in the case of *Carchesium polypinum*
326 (Templeton and Georgiadis, 1996; Zhang et al., 2006). However, there still is no universal consensus
327 about the possible biogeographic diversification of ciliates. Even if rarely, in some cases ciliates
328 population have been demonstrated to have a genetic structure related to their biogeography (Miao et
329 al. 2004; Katz et al. 2005), and this may also the case of *H. corallasia*.

330 A second scenario would be the presence of multiple cryptic species with a similar morphology, as
331 already found also in other ciliates (e.g. Strüder-Kypke and Lynn 2010; McManus et al. 2010; Kats
332 et al. 2011; Park et al. 2019). In this latter case the ITS region would result as inappropriate to
333 distinguish between closely related species, whereas the COI divergence could be explained by the
334 presence of different species living in the three localities. Indeed, the COI genetic distances within
335 *H. corallasia* are comparable or higher than the interspecific divergences within the other genera

336 [included in the analyses and show, for instance, patterns similar to those of some *Blepharisma*](#)
337 [species, which are well resolved with COI but not with ITS sequences. Moreover, Maldivian samples](#)
338 [are more similar to Caribbean ciliates rather than the Red Sea ones. This seems to contradict the](#)
339 [scenario of a circumtropical species with a biogeography-related genetic structure and further support](#)
340 [the species complex hypothesis.](#)

341 [Therefore,](#) the morphological and molecular data obtained in this work seem to support more the
342 latter scenario, with the identification of a *H. corallasia* species complex as the pathogen associated
343 to both the Caribbean Ciliate Infection and Skeletal Eroding Band. Even though it cannot be excluded
344 that the SEB may be sympatric with the CCI in some localities, this would represent an unlikely
345 scenario. The most cautious approach when describing coral diseases would be to proceed with the
346 classification of different syndromes only when clear evidence is presented (Bourne et al. 2015).
347 Since we found an approximately identical morphology at micro- and macro-scale in ciliates and
348 lesions from different localities and since *H. corallasia* may actually be a complex of multiple cryptic
349 species, we believe that in order to reduce further confusion supplementary studies that will clarify if
350 CCI and SEB should be synonymized are strongly required.

352 **Acknowledgments**

353 SM is grateful to Naturalis Biodiversity Center for providing Martin Fellowships, which supported
354 fieldwork in Curaçao (2017) and Bonaire (2019). The fieldwork in Bonaire was also supported by a
355 grant from the WWF-Netherlands Biodiversity Fund to BWH. The staff of CARMABI Marine
356 Research Center at Curaçao is thanked for logistical support. We are grateful to STINAPA and DCNA
357 at Bonaire for assistance in the submission of the research proposal and the research permit.

359 **Figure Legends**

360 **Fig. 1** Sampling localities in the Caribbean Sea (Curaçao and Bonaire), Red Sea (Saudi Arabia), and
361 Indo-Pacific (Republic of the Maldives).

362

363 **Fig. 2** *Halofolliculina* Ciliate Infection. a CCI affecting *Diploria labyrinthiformis*; b SEB affecting a
364 coral of *Acropora muricata*; c close-up of halofolliculinids on a septum of *Eusmilia fastigiata*; d
365 close-up of halofolliculinids on a colony of *Acropora muricata*. LC= live coral; DC= dead coral; the
366 arrowheads indicate the cluster-like band of protozoans

367

368 **Fig. 3** Various features of *Halofolliculina corallasia* and the peculiar single sculpture (S) of the lorica
369 (Lor) in the three investigated areas: a-b) Indo-Pacific; c-d) Red Sea; e-f) Caribbean. Scale bars: 20
370 μm

371

372 **Fig. 4** Mean values and SE of the neck diameter, neck length and the neck brim diameters of the
373 *Halofolliculina* loricae affecting Indo-Pacific (Maldives and Red Sea) and Caribbean scleractinians.
374 Mean values are expressed in μm .

375

376 **Fig. 5** Scanning Electron Microscopy Images of Caribbean skeletal eroding pattern. **a** cluster of
377 *Halofolliculina* ciliates on septae of *Diploria labyrinthiformis*; **b** close-up of loricae apparently
378 eroding the host skeleton. **c** the white dashed line show the eroding pattern left by *Halofolliculina*
379 ciliates on a colony of *Diploria labyrinthiformis*; **d** the round-shaped footprint of the loricae
380 settlement observed on the same host; **e** apparently different eroding patterns associated to
381 halofolliculinids; **f** black dashed line show slight footprints related to the presence of halofolliculinids.
382 Scale bars: a 1 mm, b 0.5 mm, c-d 50 μm , e 10 μm , f 20 μm)

383

384 **Fig. 6** Phylogenetic trees of *Halofolliculina* and relatives based on the ITS (a) and COI (b). Numbers
385 at nodes show the Bayesian posterior probabilities and the ML bootstrapping values, respectively. ‘*’
386 indicates that a node is fully supported by both analyses. Halofolliculinids from different localities are

387 highlighted with different shades of yellow; other genera are highlighted in grey. RS: Red Sea; IN:
388 Indo-Pacific; CS: Caribbean Sea.

389

390 Tables

391 **Table S1.** Measurements of the diameter, length and width of both the neck and the ampulla of
392 *Halofolliculina corallasia*’ loricae

393

394 **Table S2.** Pairwise comparisons of genetic distance values (uncorrected *p*-distances in %) within and
395 between heterotrich genera and species based on ITS and COI.

396

397 References

398 Aeby GS, Ushijima B, Campbell JE, Jones S, Williams GJ, Meyer JL, Häse C, Paul VJ (2019)
399 Pathogenesis of a tissue loss disease affecting multiple species of corals along the Florida Reef Tract.
400 Front Mar Sci 6:678.

401

402 Antonius, A. (1999). *Halofolliculina corallasia*, a new coral-killing ciliate on Indo-Pacific reefs. Coral
403 Reefs 18: 300.

404

405 Antonius, A.A., Lipscomb, D. (2001). First protozoan coral-killer identified in the Indo-Pacific. Atoll
406 Res. Bull. 481:1–21

407

408 Beli E, Aglieri G, Strano F, Maggioni D, Telford MJ, Piraino S, Cameron CB (2018) The zoogeography
409 of extant rhabdopleurid hemichordates (Pterobranchia: Graptolithina), with a new species from the
410 Mediterranean Sea. Invertebr. Syst. 32: 100-110

411

412 Bourne DG, Garren M, Work TM, Rosenberg E, Smith GW, et al. (2009) Microbial disease and the
413 coral holobiont. Trends Microbiol. 17: 554–562.

414

415 Bourne, D. G., Ainsworth, T. D., Pollock, F. J., & Willis, B. L. (2015). Towards a better understanding
416 of white syndromes and their causes on Indo-Pacific coral reefs. Coral Reefs 34: 233-242.

417

418 Bruno JF, Selig ER (2007) Regional decline of coral cover in the Indo-Pacific: timing, extent, and
419 subregional comparisons. PLoS ONE 2: e711

420

421 Casamatta DA, Stani D, Gantar M, Richardson LL (2012) Characterization of *Roseofilum reptotaenium*
422 (Cyano bacteria, Oscillatoriales) gen. et sp. nov. isolated from Caribbean black band disease.
423 Phycologia 51:489-499

424

425 Castresana, J. (2000). Selection of conserved blocks from multiple alignments for their use in
426 phylogenetic analysis. Mol Biol Evol 17: 540-552.

427

428 Cróquer, A., Bastidas, C., Lipscomb, D., Rodríguez-Martínez, R. E., Jordan-Dahlgren, E., Guzman, H.
429 M. (2006a). First report of folliculinid ciliates affecting Caribbean scleractinian corals. Coral Reefs
430 25: 187-191.

431
432 Cróquer, A., Bastidas, C., Lipscomb, D. (2006b). Folliculinid ciliates: a new threat to Caribbean corals?
433 Dis. Aquat. Org 69: 75-78.
434
435 Darriba, D., Taboada, G. L., Doallo, R., Posada, D. (2012). jModelTest 2: more models, new heuristics
436 and parallel computing. Nature Methods 9:772
437
438 Dumontier, M., & Hogue, C. W. (2002). NBLAST: a cluster variant of BLAST for NxN comparisons.
439 BMC Bioinformatics 3: 13.

440 Fernandes, N. M., da Silva Paiva, T., da Silva-Neto, I. D., Schlegel, M., Schrago, C. G. (2016). Expanded
441 phylogenetic analyses of the class Heterotrichea (Ciliophora, Postciliodesmatophora) using five
442 molecular markers and morphological data. Mol. Phylogenet. Evol 95: 229-246.
443
444 Gardener T, Cote IM, Gill JA, Grant A, Watkinson AR (2003) Long-term region-wide declines in
445 Caribbean corals. Science 301: 958–960.
446
447 Hoeksema BW, Koh EGL (2009) Depauperation of the mushroom coral fauna (Fungiidae) of
448 Singapore (1860s–2006) in changing reef conditions. Raffles Bull Zool Suppl 22:91–101
449
450 Katoh, K., Standley, DM (2013). MAFFT multiple sequence alignment software version 7:
451 improvements in performance and usability. Mol Biol Evol 30: 772-780.
452
453 Katoh, K., Misawa, K., Kuma, K. I., Miyata, T (2002) MAFFT: a novel method for rapid multiple
454 sequence alignment based on fast Fourier transform. Nucleic Acids Res 30: 3059-3066.

455 Katz LA, DeBerardinis J, Hall MS, Kovner AM, Dunthorn M, Muse SV (2011) Heterogeneous rates of
456 molecular evolution among cryptic species of the ciliate morphospecies *Chilodonella uncinata*.
457 Journal of molecular evolution 73: 266-272.

458
459 Kumar S, Stecher, G, Li M, Knyaz C, Tamura K (2018) MEGA X: Molecular Evolutionary Genetics
460 Analysis across Computing Platforms. Mol Biol Evol 35: 1547-1549.
461
462 McManus, G. B., Xu, D., Costas, B. A., & Katz, L. A. (2010). Genetic identities of Cryptic species in
463 the *Strombidium stylifer/apolatum/oculatum* cluster, including a description of *Strombidium*
464 *rassoulzadegani* n. sp. Journal of eukaryotic microbiology 57: 369-378.
465
466 Meyer JL, Castellanos-Gell J, Aeby GS, Häse C, Ushijima B, Paul VJ (2019) Microbial community
467 shifts associated with the ongoing stony coral tissue loss disease outbreak on the Florida Reef Tract.
468 bioRxiv 626408
469
470 Miller MA, Holder MT, Vos R, Midford PE, Liebowitz T, Chan L, Warnow T (2009) The CIPRES
471 portals.
472
473 Montano S, Arrigoni R, Pica D, Maggioni D, Puce S. (2015). New insights into the symbiosis between
474 *Zanclaea* (Cnidaria, Hydrozoa) and scleractinians. Zool Scripta 44: 92-105
475
476 Page CA, Willis BL (2008) Epidemiology of skeletal eroding band on the Great Barrier Reef and the
477 role of injury in the initiation of this widespread coral disease. Coral Reefs 27: 257-272.
478

479 Page C A, Cróquer A, Bastidas C, Rodríguez S, Neale SJ, Weil E, Willis BL (2015) *Halofolliculina*
480 ciliate infections on corals (skeletal eroding disease). In: Woodley CM, Downs CA, Bruckner AW,
481 Porter JW, Galloway SB (eds.) *Diseases of Coral*, Wiley-Blackwell, Hoboken, pp 361-375.
482
483 Park, M. H., Jung, J. H., Jo, E., Park, K. M., Baek, Y. S., Kim, S. J., & Min, G. S. (2019). Utility of
484 mitochondrial CO1 sequences for species discrimination of Spirotrichea ciliates (Protozoa,
485 Ciliophora). *Mitochondrial DNA Part A* 30: 148-155.
486
487 Pollock FJ, Morris PJ, Willis BL, Bourne DG (2011) The urgent need for robust coral disease
488 diagnostics. *PLoS Pathogens* 7(10):e1002183
489
490 Primc-Habdija, B., Matoničkin, R. (2005). A new freshwater folliculinid (Ciliophora) from the karstic
491 region of Croatia. *Eur J Protistol* 41:, 37-43.
492
493 Rambaut A. (2012). Figtree v 1.4.0. <http://tree.bio.ed.ac.uk/software/figtree/>
494
495 Richardson LL (1998) Coral diseases: what is really known? *Trends Ecol. Evol.* 13: 438–443.
496
497 Riegl B, Antonius A (2003) *Halofolliculina* skeleton eroding band (SEB): a coral disease with
498 fossilization potential? *Coral Reefs* 22:48
499
500 Rodríguez S, Croquer A, Guzmán HM, Bastidas C (2009) A mechanism of transmission and factors
501 affecting coral susceptibility to *Halofolliculina* sp. infection. *Coral reefs* 28: 67-77.
502
503 Ronquist F, Teslenko M, van der Mark P, Ayres DL, Darling A, Höhna S, Larget B, Liu L, Suchard
504 MA, Huelsenbeck JP. 2012. MrBayes 3.2: efficient Bayesian phylogenetic inference and model
505 choice across a large model space. *Syst. Biol.* 61: 539-542.
506
507 Rosenberg E, Kelloff CA, Rohwer F (2007) Coral microbiology. *Oceanography* 20: 146–154.
508
509 Sutherland WJ, Clout M, Depledge M, Dicks LV, Dinsdale J, Entwistle AC, Fleishman E, Gibbons DW,
510 Keim B, Lickorish FA, Monk KA, Ockendon N, Peck LS, Pretty J, Rockström J, Spalding MD,
511 Tonnejck FH, Wintle BC (2015) A horizon scan of global conservation issues for 2015. *Trends Ecol.*
512 *Evol.* 30:17–24.
513
514 Sussman M, Bourne DG, Willis BL (2006) A single cyanobacterial ribotype is associated with both red
515 and black bands on diseased corals from Palau. *Dis. Aquat. Organ.* 69: 111-118
516
517 Stamatakis A (2006) RAxML-VI-HPC: maximum likelihood-based phylogenetic analyses with
518 thousands of taxa and mixed models. *Bioinformatics* 22: 2688-2690.
519
520 Stamatakis A (2014) RAxML version 8: a tool for phylogenetic analysis and post-analysis of large
521 phylogenies. *Bioinformatics* 30: 1312-1313.
522
523 Strüder-Kypke MC, Lynn DH (2010) Comparative analysis of the mitochondrial cytochrome c oxidase
524 subunit I (COI) gene in ciliates (Alveolata, Ciliophora) and evaluation of its suitability as a
525 biodiversity marker. *Syst Biodivers* 8: 131-148.
526
527 Sun P, Clamp JC, Xu D (2010) Analysis of the secondary structure of ITS transcripts in peritrich ciliates
528 (Ciliophora, Oligohymenophorea): Implications for structural evolution and phylogenetic
529 reconstruction. *Mol Phylogenet Evol* 56: 242–251

530
531 Sweet JM, Séré GM (2015) Ciliate communities consistently associated with coral diseases. *J Sea Res*
532 113: 119-
533
534 Talavera G, Castresana J (2007) Improvement of phylogenies after removing divergent and
535 ambiguously aligned blocks from protein sequence alignments. *Syst Biol*, 56 564-577.
536
537 Weil E, Hooten, AJ (2008) Underwater cards for assessing coral health on Caribbean reefs. *Coral reefs*
538 targeted research and capacity building for management, 24-pp.
539
540 Weil E, Rogers CS (2011) Coral reef diseases in the Atlantic-Caribbean. In: Dubinsky Z, Stambler N
541 (eds.) *Coral Reefs: An Ecosystem in Transition* Springer, Dordrecht, Netherlands, pp 465–491
542
543 Willis BL, Page CA, Dindsdale EA (2004) Coral disease in the great barrier reef. In: Rosenberg E, Loya
544 Y (eds) *Coral health and disease*. Springer, Berlin, pp 69–104
545
546 Winkler R, Antonius A, Abigail Renegar, D. (2004) The skeleton eroding band disease on coral reefs of
547 Aqaba, Red Sea. *Mar Ecol* 25: 129-144.
548
549 Woodley, Cheryl M.; Downs, Craig A.; Bruckner, Andrew W.; Porter, James W.; Galloway, Sylvia B.
550 (2016). *Diseases of Coral*. Wiley-Blackwell, Hoboken,
551
552 Work T, Meteyer C (2014) To understand coral disease, look at coral cells. *EcoHealth* 11: 610-618.
553
554 Yi Z, Song W (2011) Evolution of the order Urostylida (Protozoa, Ciliophora): new hypotheses based
555 on multi-gene information and identification of localized incongruence. *PLoS ONE* 6, e17471.
556
557 Zar JH (1999) *Biostatistical analysis*. Prentice-Hall, London
558